

Review Article

Methodological aspects of *in vivo* axial loading in rodents: a systematic review

Ashwini Kumar Nepal¹, Hubertus W. van Essen¹, Renate T. de Jongh², Natasja M. van Schoor³, René H.J. Otten⁴, Dirk Vanderschueren⁵, Paul Lips², Nathalie Bravenboer¹

¹Department of Clinical Chemistry, Amsterdam UMC, Vrije Universiteit Amsterdam, Amsterdam Movement Sciences, Amsterdam, The Netherlands;

²Department of Internal Medicine, Endocrine section, Amsterdam UMC, Vrije Universiteit Amsterdam, Amsterdam, The Netherlands;

³Department of Epidemiology and Biostatistics, Amsterdam Public Health Research Institute, Amsterdam UMC, Vrije Universiteit Amsterdam, Amsterdam, The Netherlands;

⁴Medical Library, Vrije Universiteit Amsterdam, Amsterdam, The Netherlands;

⁵Department of Chronic Diseases, Metabolism and Ageing, Laboratory of Clinical and Experimental Endocrinology, KU Leuven, Leuven, Belgium

Abstract

Axial loading in rodents provides a controlled setting for mechanical loading, because load and subsequent strain, frequency, number of cycles and rest insertion between cycles, are precisely defined. These methodological aspects as well as factors, such as ovariectomy, aging, and disuse may affect the outcome of the loading test, including bone mass, structure, and bone mineral density. This review aims to overview methodological aspects and modifying factors in axial loading on bone outcomes. A systematic literature search was performed in bibliographic databases until December 2021, which resulted in 2183 articles. A total of 144 articles were selected for this review: 23 rat studies, 74 mouse studies, and 47 knock out (KO) mouse studies. Results indicated that peak load, frequency, and number of loading cycles mainly affected the outcomes of bone mass, structure, and density in both rat and mouse studies. It is crucial to consider methodological parameters and modifying factors such as age, sex-steroid deficiency, and disuse in loading protocols for the prediction of loading-related bone outcomes.

Keywords: Axial Loading, Bone, Rats, Mice, Mechanical Stress

Introduction

Bone tissue adapts to mechanical forces endured during growth, locomotion, and physical activities¹. High impact loading activities such as weightlifting, tennis, squash or badminton are more osteogenic than swimming, cycling or running², because bone cells respond better to high strain changes at fast rates with an unusual distribution.

This can be explained by the mechanostat-theory proposed by Frost³⁻⁶, who postulated that several mechanical thresholds determine whether old bone is resorbed or new bone is formed⁴. Mechano-adaptation is considered as an important function of bone and is therefore used as an outcome in several studies. Several invasive⁷, *in vitro*⁸, and non-invasive *in vivo*⁷ mechanical loading models have been reported previously to investigate mechano-adaptation. Non-invasive loading is preferred because it reduces surgical artifact⁷. These non-invasive models include axial compression of the ulna or tibia, four-point bending of the tibia⁹, and the cantilever bending of the tibia¹⁰. Of the different models, axial compression of rodent long bones best simulates locomotor bone loading patterns, engenders physiologically relevant strains during short bouts of loading, and allows assessment of the loading-related response throughout the whole bone^{11,12}. Moreover, it enables the study of mechanical loading in a controlled

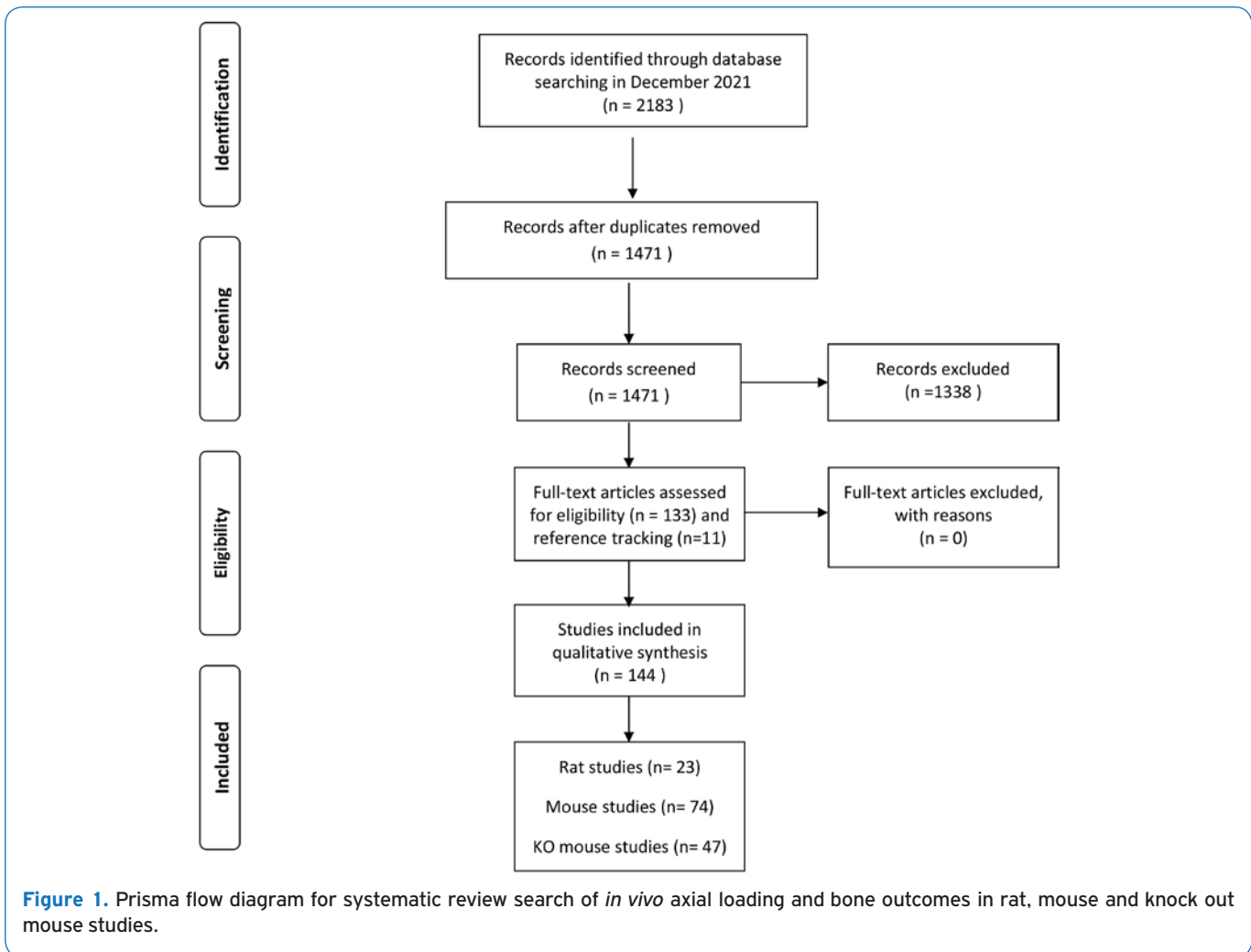
The authors have no conflict of interest.

Corresponding author: Dr. Nathalie Bravenboer, PhD, Department of Clinical Chemistry, Amsterdam UMC, Vrije Universiteit Amsterdam, PO Box 7057, 1007 MB, Amsterdam, The Netherlands
E-mail: n.bravenboer@amsterdamumc.nl

Edited by: G. Lyrakis

Accepted 17 March 2023





setting because load, frequency, duration of the loading, and rest period can be defined.

Each laboratory designs its own protocol, with reference to the choice of species, preparation of custom-designed molds for holding the bone in the load cell, the appropriate peak load, frequency, number of cycles, rest insertion between cycles, and the duration of the loading sessions. All these methodological aspects of loading protocols can influence outcomes of bone mass, structure, and density and thereby potentially determine the conclusion on mechano-adaptation. Axial loading has been widely used in studies with knock out mouse models. This makes the impact of different aspects of a loading regime on bone outcome indices highly relevant. There are several overviews of non-invasive loading models and their implications on aging, mechanosensitivity and subsequent bone adaptation. However, these have not taken the different methodological aspects of loading into account with respect to bone outcomes^{7,11-13}.

The main objective of this systematic review was to study the effects of methodological aspects of non-invasive *in vivo*

axial compression loading in rat, mouse and knock out mouse studies on bone mass, structure, and density. In addition, we aimed to examine the influence of modifying factors like age, sex-steroid deficiency and disuse.

Methods

Search strategy

This systematic review used the Preferred Reporting Items for Systematic reviews and Meta-Analysis (PRISMA) checklist¹⁴. The literature search was performed in the bibliographic databases PubMed, Embase, and SPORTdiscus (via EBSCO) from the start of these databases to Dec 31, 2021. The following keyword search was used: “mechanical loading” AND “ulna” or “tibia” AND “rats” or “mice” AND “bone density.” Search terms included controlled terms (e.g. MeSH in PubMed) as well as free text terms for all six concepts. Only non-invasive *in vivo* axial loading studies in rats and mice and knock-out mouse models that studied bone outcomes (bone mass, structure, and density) were

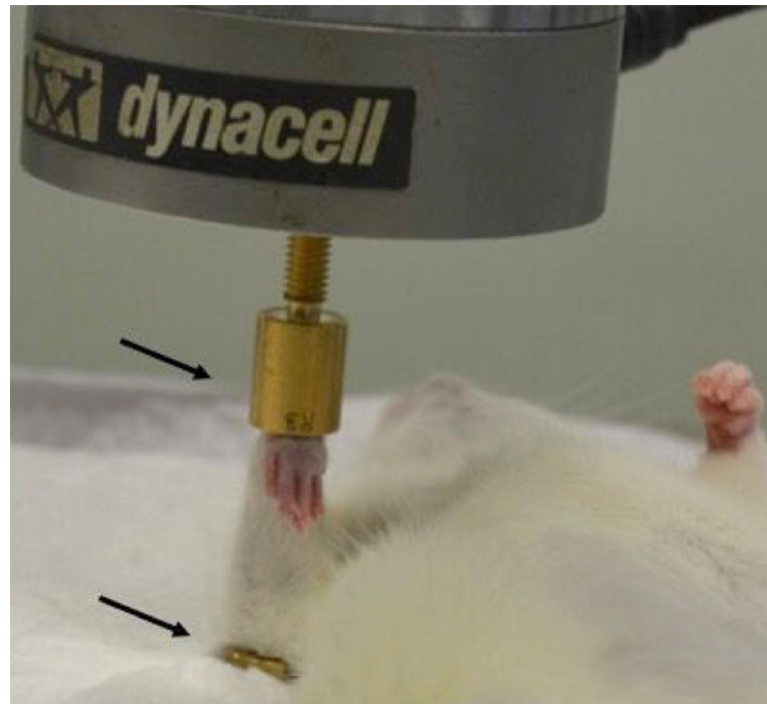


Figure 2. Rat ulna held in custom-made cups (arrows) during an *in vivo* axial loading experiment on the Instron device. The two arrows represent upper and lower custom-made cups.

included. The flow chart for the selection steps of the articles is presented in Figure 1.

Study selection

Two authors (N.B. and H.E.) independently selected relevant titles from the electronic databases. The discrepancies that arose from the two independent authors were resolved by consensus after reading the abstracts and full text of selected titles. The following inclusion criteria were used: (a) intervention: *in vivo* axial mechanical loading, (b) outcome measurements: bone mass, bone volume, bone mineral density, and (c) rats or mice (d) tibia or ulna.

Experimental animals

The search regarded axial loading studies in the following rat species: Sprague Dawley, Wistar, Fischer, and mouse species: C57BL/6, BALB/c, DBA/2, C3H/He, CD1. Knock-out mouse model studies selected in this review were used to examine the effect of axial loading on genetically modified mice.

Loading protocols

We searched papers on the axial loading of ulna or tibia. Although most investigators used in house developed methods, in general, load was applied using a dynamic

loading device: Instron (Instron, Norwood, MA USA), MTS (MTS, Eden Prairie, MN USA), Electroforce (TA Instruments, New Castle, DE USA) or Zwick testing device (ZwickRoell LP, Kennesaw, GA USA), connected to a computer in which the loading cycles are electronically recorded. Custom-made cups are adapted to hold ulna or tibia on the loading device for *in vivo* loading experiments. An example of rat ulna loaded in custom made cups on the Instron device is presented in Figure 2. A single loading cycle is the duration required for the load to ascend, reach its peak, and slowly descend to its initial level. A single loading bout consists of several loading cycles. In a typical axial loading experiment, rats or mice are anesthetized, ulna or tibia are held in custom loading cups, peak load is applied at a certain frequency, number of cycles in a single bout or multiple loading sessions. The variables used in the *in vivo* axial loading experiment include the peak load, strain rate, loading waveforms, frequency, number of loading cycles, rest period between cycles, and the duration of loading sessions. Loading protocols are designed by customizing the parameters to deliver the desired loading regimen, which differs according to the study rationale. The animals are anesthetized just before the loading experiment, and remain sedated until completion. Both inhalation-based anesthesia, such as 1-2% isoflurane or 1.5-3% halothane, and injectable anesthesia: a combination of ketamine 60-150 mg/kg body weight and α -2 adrenoreceptor agonists such as

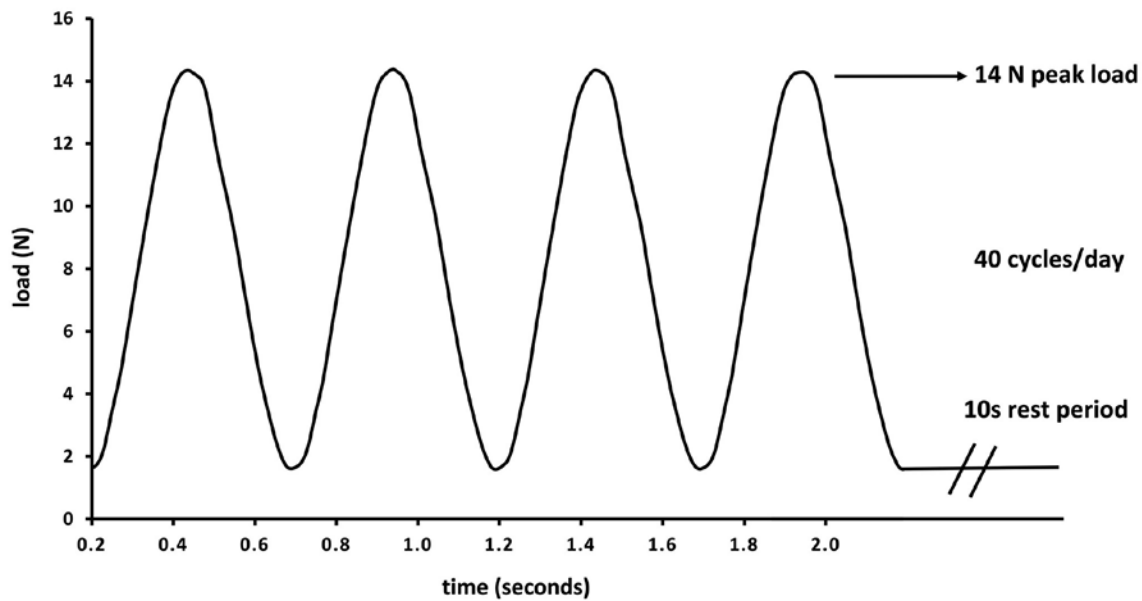


Figure 3. An example of axial loading protocol in rat ulna with 14 N peak load and 10s rest periods between cycles for 40 cycles.

xylazine 7.5-20 mg/kg body weight or medetomidine 0.4-1 mg/kg body weight can be used in mouse or rat studies¹⁵. The latter is commonly used because inhalation-based anesthesia requires specialized equipment and training. For quick recovery from sedation after the loading experiment, α -2-adrenocortical antagonist atipamezole (1 mg/kg) is injected¹⁵. After applying sedation, first the tibia or ulna of the rodent is placed in the custom-made cup to stabilize it with a 0.5 N-1 N preload. This is recommended for proper stabilization of the bone in the loading apparatus^{7,16}. The peak load corresponding to the peak compressive strain can be calculated by *ex vivo* load-strain calibration in cadaveric bones. The load is applied between the flexed carpus and olecranon joints in the ulna, and between the knee and ankle joints in the tibia. The peak load results in peak compressive strain, and can be applied cyclically to ensure maximum bone formation. For optimum bone formation, the peak compressive strain should not exceed the yield point at which damage occurs to the bone, and should be lower than the fatigue load which causes microdamage to the bone^{7,11,13}. Strain rate is the change in strain per unit time¹⁷. Strain varies at different bone locations in both rat and mouse tibia and ulna¹⁸⁻²⁰. Site-specific measurement of strain in proximal, medial, and lateral sites of the tibia using *in vivo* micro CT and finite element models, and digital image correlations has been performed^{18,21}. These methods have shown to be more reproducible than using strain gauges and eliminates the sacrifice of animals for this measurement. The axial load is applied for a specific duration which consists of multiple loading cycles on the same day^{22,23}, or it is repeated for three to five days a week for two to six weeks^{16,24,25}. Multiple loading

waveforms are used, such as sinusoidal or haversine, and non-sinusoidal: trapezoid, triangular, or sawtooth waveform²⁶. The loading frequency usually corresponds to the normal stride frequency during locomotion, also represented as the number of cycles per unit time¹⁷. A rest period between loading cycles can be applied in loading protocols. Dynamic load is mostly applied in a sinusoidal manner on the tibia or the ulna, while the contralateral bone is kept as control. Static loading applied at low compressive strain suppresses bone formation, and is therefore not often used²⁷. An example of the rat ulna axial loading experiment with 14 N peak load and 10s rest periods between cycles for 40 cycles is presented in Figure 3.

Bone outcomes

This review restricted the outcome parameters to bone histomorphometry and micro CT, DXA, or peripheral quantitative computed tomography (pQCT).

Modifying factors

In this review, papers that possibly describe factors that might affect load induced bone formation are included. Several of these factors were investigated as potential modifying factors which include: age, sex steroids, osteoporosis treatment, and prior disuse. The effect of sex steroids was studied by ovariectomy (OVX) or orchietomy (ORX), with or without treatment with sex-steroid hormones. Tamoxifen an estrogen receptor modulator that couples agonistic effects on bone with antagonistic effects on other organs was also tested for affecting mechano-adaptation²⁸.

Table 1. Summary of rat axial loading studies.

Author/Year	Animals/ age/ bone type	Interventions	Peak load (N)	Strain ($\mu\epsilon$)	loading cycles (per day)	Frequency (Hz)/ waveform	Rest periods (seconds)	Duration of loading experiment (days or week)	Outcomes parameters
Chen 2008 ³⁷	Female Sprague Dawley rats, 12 weeks, left ulna	N/A	N/A	2000 and 3000	N/A	5, 10 and 15	N/A	2 weeks	DEXA: BMD, histomorphometry: MS/BS, MAR, BFR/BS
Feher 2010 ⁴²	Female Sprague Dawley rats	OVX, bisphosphonates	15	3000	360	2	N/A	1 week	Histomorphometry: MS/BS, MAR, BFR/BS
Hsieh 2001 ²⁰	Female Sprague Dawley rats, 28-32 weeks, right ulna	N/A	6.5, 10.5, 14.5, 18.5, 22.5	1343, 2284 and 3074	360	2, haversine	N/A	2 weeks	Histomorphometry: MS/BS, MAR, BFR/BS
Hsieh 2001 ³⁴	Female Sprague Dawley rats, 28-32 weeks, right ulna	N/A	4.3-18	360-4680	360	1, 5 and 10	N/A	2 weeks	Histomorphometry: MS/BS, MAR, BFR/BS
Ko 2012 ⁴³	Female Sprague Dawley, 12 weeks, right tibia	OVX & SHAM	N/A	2000	1500	2	N/A	2 weeks	Micro CT: trabecular bone: BV/TV
Li 2002 ³⁸	Female Sprague Dawley rats, 28 weeks, right ulna	Vehicle and oral indomethacin or NS-398	17	3600	360	2	N/A	N/A	Histomorphometry: MS/BS, MAR and BFR/BS
Li 2003 ⁴⁰	Female Sprague Dawley, 28 weeks, right ulna	Vehicle treated, verapamil and PTH	16.5	3600	360	2, haversine	N/A	N/A	histomorphometry: MS/BS, MAR, BFR/BS
Li 2021 ³³	Female Sprague Dawley rats, 26 weeks, left tibia	Pregnancy, lactation, weaning and virgin	45	1500	N/A	2	N/A	5 times a week for 2 weeks	<i>In vivo</i> micro CT: trabecular bone: BV/TV, Tb.N, Tb.Th, Tb.Sp, Conn.D, SMI, cortical bone; Ct.Ar, Ct.Th, polar moment of inertia, histomorphometry: MS/BS, MAR, BFR/BS
Mosley 1998 ¹⁷	Male Sprague Dawley, 6 weeks, left ulna	N/A	1-20	4000	1200	2, trapezoidal	N/A	2 weeks	Histomorphometry: MS/BS, MAR, BFR/BS
Mustafy 2020 ⁹⁷	Male Sprague Dawley, 4 weeks, tibia	N/A	N/A	450, 850, and 1250	1200	2, haversine waveform	0.10	5 days/week for 8 weeks	<i>In vivo</i> micro CT: trabecular bone; BMD, BV/TV, Tb.Th, Tb.N, Tb.Sp, cortical bone; TMD, T.Ar, Ct.Ar, Ct.Th, Ma.Ar, Ps.Pm, Ec.Pm, mean eccentricity, polar moment of inertia
Noble 2003 ⁹⁸	Sprague Dawley rats, left ulna	N/A	N/A	4000	1200	2	N/A	1-5 and 8-12 days inclusive	Histomorphometry: calcein labelled surface
Perry 2009 ³¹	Female Wistar, left ulna	Ultrasound	7	4000 and 4500	40	10	10	two weeks	Histomorphometry: MS/BS, MAR, BFR/BS
Robling 2001 ²⁷	Male Sprague Dawley, right ulna	N/A	17	3500	1200	2	N/A	1-5 and 8-12 days inclusive	Histomorphometry: MS/BS, MAR, BFR/BS

Table 1. (Cont. from previous page).

Author/Year	Animals/ age/ bone type	Interventions	Peak load (N)	Strain ($\mu\epsilon$)	loading cycles (per day)	Frequency (Hz)/ waveform	Rest periods (seconds)	Duration of loading experiment (days or week)	Outcomes parameters
Robling 2002 ²⁴	Female Sprague Dawley	N/A	17	3600	360	2, haversine	N/A	16 weeks	DEXA: BA, BMC, aBMD, pQCT: cortical bone; CSA, Cortical vBMD, minimum and maximum moment of inertia
Saxon 2005 ³⁵	Female Sprague Dawley, 12 weeks, right ulna	N/A	15	3288	360	2, haversine	N/A	15 weeks	Histomorphometry: MS/BS, MAR, BFR/BS pQCT: Ct.Ar, T.Ar, Cortical vBMD, second moment of inertia (Imin and Imax)
Saxon 2006 ³⁶	Male Sprague Dawley, 8 weeks, right ulna	N/A	17	4094, 4277	N/A	N/A	N/A	5 weeks	Histomorphometry: MS/BS, MAR, BFR/BS, pQCT: vBMD, second moment of inertia (Imin), BMC, Ct.Ar, periosteal and endocortical circumference
Schriefer 2005 ⁹⁹	Female Sprague Dawley rats, right ulna	N/A	9.0, 11.3 and 13.5	N/A	360	2, haversine	N/A	5 weeks	pQCT: BMC, T.Ar, second moment of inertia (Imin and Imax), histomorphometry: BFR/BS
Tomlinson 2014 ³⁹	Male Fischer, 13-14 weeks, right ulna	$\alpha\beta 3$ targeted nano-particle and vehicle treatment	15 or 18	N/A	100	0.1	N/A	N/A	Histomorphometry: MS/BS, MAR, BFR/BS, micro CT: BV/TV, BMD
Torrance 1994 ⁹	Male Sprague Dawley, left ulna	N/A	15 or 20	1828 (proximal medial), 1700 (proximal lateral), 3750 (mid shaft medial), 3125 (medial lateral)	1200	10 or 20	N/A	on days 5, 6, 8 11, 12, 13, 14 and 15	Histomorphometry: periosteal new bone formation
Warden 2005 ²⁵	Female Sprague Dawley, 18-20 weeks, right ulna	N/A	17	3600	360	2, haversine	N/A	3 days/week for 5 weeks	DXA: BMC, aBMD, pQCT: BMC, vBMD and micro CT: Ct.Ar, second moment of inertial (Imin and Imax)
Warden 2007 ⁴¹	Female Sprague Dawley, 5 weeks, right ulna,	N/A	8.5	3500	360	2, haversine	N/A	3 days/week for 7 weeks	DXA: aBMD, BMC, pQCT: Ct.Ar, second moment of inertia (Imin and Imax)
Warden 2013 ⁴⁴	Female Sprague Dawley, right ulna	OVX, sham	8.5	3500	360	2	N/A	3 days/week for 6 weeks	pQCT: vBMD, Ct.Ar, BMC, second moment of inertia (Imin and Imax), micro CT: Ct.Ar, Tt.Ar, Me.Ar, Ct.Th, Imin
Yang 2018 ⁴⁵	Sprague Dawley rats, 20 weeks	Hindlimb unloading and controls	20	800	600	1	N/A	5 days/week for 4 weeks	Micro CT: trabecular bone; BV/TV, Tb.Sp, Tb.Th, Tb.N, bone volume surface ration (BSV/BV) cortical bone; Ct.Th, DEXA: BMD and BMC

Osteoporotic bone loss was often treated with a bone sparing medication. Bisphosphonates²⁹, and intermittent parathyroid hormone (iPTH) were included to test the effect on load induced bone formation³⁰. Ultrasound exposure improves fracture healing by affecting cellular mechanisms such as inflammatory responses involved in the fracture healing process. Therefore, ultrasound exposure was also included as a potential modifying factor³¹. Disuse was induced by sciatic neurectomy, causing paralysis and immobilization of the limb³².

Results

The systematic search resulted in 2183 potentially eligible articles. The search included 905 articles from Pubmed, 1207 from Embase, and 71 from SPORTdiscus (via EBSCO). After duplicates were removed, 1471 articles remained. Among the search results, 1222 articles were excluded by both reviewers, since they did not meet the inclusion criteria resulting in 249 articles. Since consensus on 59 articles was missing, the abstract and the full texts were read for 249 articles, resulting in another exclusion of 116 articles and the inclusion of 133 articles (Figure 1). Reference tracking led to the inclusion of 11 additional articles, resulting in a total of 144 articles for final analysis. The agreement between the two reviewers was good (Cohen's Kappa=0.76). Of the 144 articles selected for the review, 23 articles concerned rat studies, 74 concerned mouse studies, and 47 concerned KO mouse studies (Figure 1).

Mechanical loading protocols and modifying factors affecting bone outcomes in rats

Twenty-three articles concerning rat studies are summarized in Table 1. In rat ulna axial loading studies, peak load ranged from 4.3 to 22.5 N and strain ranged from 360 $\mu\epsilon$ to 4680 $\mu\epsilon$. One rat study applied a peak load on the tibia of 45 N, corresponding to a strain of 1500 $\mu\epsilon$ ³³. In all rat studies, load-strain was calibrated using a strain gauge to calculate the strain. Frequencies and number of cycles ranged from 1.5 Hz to 15 Hz and 40 to 1500 cycles per day. A loading session that was repeated three times a week for two to five weeks was reported frequently^{20,25,31,34-37}, but two studies performed a single duration loading experiment^{38,39}. A rest period of 10s between loading cycles was applied in one rat axial study³¹. One study compared rats of 3 groups, i) loaded 1st session of 5 weeks followed by 10 week rest (1x5), ii) loaded 1st and 3rd sessions of 5 weeks each with 5 weeks recovery period (2x5), and iii) loaded all 3 sessions of 5 weeks each (3x5) without recovery period with two control groups: one age-matched control group received no loading or anesthesia, and one control group sacrificed at baseline. This study reported an increase in bone formation parameters: mineralizing surface (MS/BS), bone formation rate (BFR/BS) and mineral apposition rate (MAR) for all three groups in the first five weeks as compared to controls³⁵. However, only the 2x5 group showed improved bone formation as compared to

controls after 15 weeks³⁵. Two studies tested axial loading with increasing peak loads of 6.5-18.5 N²⁰ and 4.3-18.0 N³⁴ and showed that with increasing peak loads periosteal bone formation occurred in a dose-dependent manner^{20,34}. The compressive strain varied with the diaphyseal location, which increased from proximal to distal region in the tibia, and periosteal bone formation also increased distally³⁴. However, a clear dose-response was not observed on the endocortical surface³⁴. The strain threshold, when peak strain magnitude attained during the loading session exceeds that of habitual activity and subsequently bone formation occurs, is also referred as the minimal effective strain (MES)⁴⁻⁶. Dynamic load, like a cyclic load improved bone outcomes, more than a static load, or constant load. This is true especially for the histomorphometric bone formation parameters BFR/BS, MS/BS and MAR, which, compared to controls, were suppressed or unaffected in periosteal and endocortical surfaces after static load but increased after dynamic load in both periosteal and endocortical surfaces²⁷. The frequency of axial loading was shown to be an important determinant, for bone mineral density (BMD). A frequency of 10 Hz and 15 Hz showed a mechanical loading-related increase in ulnar BMD after two weeks while 5 Hz did not³⁷. However, their study did not compare BMD in frequencies above 10 Hz and 15 Hz, so it could not be concluded whether frequencies above 10-15 Hz affected BMD. A rat axial loading study that used 1, 5 and 10 Hz frequency at peak loads of 4-18 N showed that increased loading frequency increased the slopes of peak strain versus rBFR/BS and rMS/BS curves, indicating that the increase in loading frequency enhanced loading-induced bone formation³⁴.

Although the choice of rat species, mostly female Sprague Dawley (SD) rats^{20,24,25,34,35,37,40-43}, varied with the design of *in vivo* axial loading, it did not seem to affect the bone outcomes. One study reported that load induced bone formation was not different in six-month old rats as compared to ten-month old rats after two weeks of axial loading³⁵. Axial loading related bone formation response was not different in bisphosphonate-treated OVX rats, as compared to OVX alone⁴². Another OVX rat axial loading study reported that load-related skeletal maintenance was not affected by OVX, and no significant interactions were observed between OVX and loading⁴⁴. Axial loading was also studied during disuse, using a hind-limb unloading model, where axial loading did not affect BMD as compared to age-matched controls after 21 days and 28 days⁴⁵. Drug treatment with verapamil or prednisolone inhibited bone formation^{40,46}, whereas, PTH supplementation⁴⁰ and ultrasound exposure³¹ increased bone formation. The different characteristics and protocols of studies with rat axial loading are summarized in Table 1.

Mechanical loading protocols and modifying factors affecting loading related bone outcomes in mouse and knock-out mouse models

Seventy-four articles which concerned mouse studies and 47 articles which concerned knock out mouse studies are

Table 2. Summary of mouse axial loading studies.

Author/Year	Animals/age/ loaded bone	Interventions	Peak loads (N)	Strain ($\mu\epsilon$)	loading cycles (per day)	Frequency (Hz)/waveform	Rest periods (seconds)	Duration of loading experiment (days or week)	Outcomes
Bergstrom 2018 ⁴⁶	Female C57BL/6J mice, 12 weeks old, right tibiae	Prednisolone treatment and vehicle	13	3091	40	Trapezoid waveform	10	3 days/week for 2 weeks	pQCT: trabecular bone: Tb.vBMD, cortical bone: cortical thickness, Ct.BMC, periosteal perimeter, endocortical perimeter, moment of inertia, moment of resistance
Berman 2015 ⁴⁸	Female C57BL/6 mice, 12 weeks, right tibiae	N/A	8.8, 10.6 or 12.4	1700, 2050 and 2400	220	N/A	N/A	2 weeks	Micro CT: trabecular bone: BV/TV, Tb.Th, Tb.N, Tb.Sp, SMI, cortical bone: Ct.Ar, Ct.Th, Ma.Ar, Ec.Pm. moment of inertia
Berman 2019 ¹⁰⁰	Male C57BL/6J mice, 3 months old, right tibiae	N/A	11.9	N/A	220	4	1	3 weeks	Micro CT: trabecular bone: BV/TV, BMD, Tb.Th, Tb.N, Tb.Sp, cortical bone: T.Ar, Ct.Ar, Ma.Ar, Ct.Ar/Tt.Ar, TMD Ct.Th, Ps.Pm, Ec.Pm, principal moment of inertia, TMD
Bouchard 2021 ⁷⁹	Female C57BL/6J mice, 10 weeks old, left tibiae	N/A	11.0	1200	216	4	N/A	5 days per week for 2 weeks	Histomorphometry: MS/BS, MAR, BFR/BS, micro CT: cortical bone: Ct.Ar, Tt.Ar, Ct.Ar/Tt.Ar, Ct.Th, Ct.vTMD, trabecular bone: BV/TV, Tb.Th, Tb.N, Tb.Sp, Tb.vTMD
Cheong 2021 ¹⁰¹	Female C57BL6/J mice, 14 weeks, right tibiae	OVX	12	N/A	40	N/A	N/A	3 days/ per week for 3 weeks	Micro CT: BV, BMC, BV/TV, BMD
Cheong 2020 ¹⁰²	Female C57BL6/J mice, 14 weeks, right tibiae	OVX	2-12	1500	40	Trapezoid waveform	10	3 days/ per week for 3 weeks	Micro CT: BMC, BMD
Cheong 2021 ¹⁰³	Female C57BL6/J mice, 13 weeks, right tibiae	OVX, PTH	2-12	1500-2000	40	Trapezoid waveform	10	3 days/ per week for 3 weeks	Micro CT: BV, BV/TV, BMC, BMD
DeLong 2020 ¹⁰⁴	Male C57BL/6J mice, 16 weeks, right tibiae	N/A	9	N/A	1200	4	N/A	4 days/ week for 21 weeks	Micro CT: trabecular bone: TV, BV/TV, TbN, Tb.Th, Tb.Sp, Conn.D, SMI, and BMD, cortical bone: TV, total BV, CtBV/TV, Ct.Th, Ma.Ar, Ct.Po, TMD
Fioravanti 2021 ¹⁰⁵	C57BL/6J mice, right tibia	Gambogic amide or VEH	3	N/A	100	2	N/A	N/A	Histomorphometry: MS/BS, MAR, BFR/BS
Fritton 2005 ⁶²	Male C57BL/J	N/A	3	800	1200	N/A	0.1 (every 4 cycles)	2 weeks to 6 weeks	Histomorphometry: MS/BS, MAR, BFR/BS, micro CT: BMC, BV, TV, BV/TV, Tb.Th, Tb.Sp
Galea 2020 ⁷⁸	Female and male C57BL/6J mice, 19 weeks and 19 month, right tibia	Aging, sciatic neurectomy	14.5	2270	40	Trapezoid waveform	10	3 alternate days for 2 weeks	Micro CT: trabecular bone: BV/TV, Tb.Th, Tb.N, Tb.Sp, Tb.Pf, SMI cortical bone: T.Ar, Ct.Ar, B.Ar/T.Ar, Ma.Ar, Cs.Th, Ct.Po, polar moment of inertia
Gohin 2020 ¹⁰⁶	Male C57BL/6 mice, 10-12 weeks, right tibia	N/A	12	N/A	40	2	10	3 days/ week for 2 weeks	micro CT: trabecular bone: BV/TV, Tb.Th, Tb.Sp, Tb.N, Tb.Pf, SMI, cortical bone: Tt.Ar, Tt.Pm, Ct.Ar, Ct.Th, polar moment of inertia
Holguin 2013 ⁴⁹	Female C57BL/6, BALB/c, 16 weeks, right tibiae	N/A	10	2800 (C57BL/6), 2350 (BALB/c),	WashU: 60, Cornell/ HSS: 1200	N/A	WashU: 10s Cornell/ HSS: 0.1s 0.1s rest insertion,	3 days/week for 6 weeks	<i>In vivo</i> micro CT: cortical bone: BV, Tt.Ar, Ma.Ar, Ct.Th, andTMD), trabecular bone: BV/TV, Tb.Th, Tb.N, and vBMD

Table 2. (Cont. from previous page).

Author/Year	Animals/age/ loaded bone	Interventions	Peak loads (N)	Strain ($\mu\epsilon$)	loading cycles (per day)	Frequency (Hz)/waveform	Rest periods (seconds)	Duration of loading experiment (days or week)	Outcomes
Ko 2016 ¹⁰⁷	Male C57BL/6, BALB/c, 26 weeks, left tibia	NA	9	800	1200	4	N/A	3 times per week for 2 weeks	Micro CT: trabecular bone: BV/TV, Tb.Th, and Tb.Sp
Kuruville 2008 ¹⁹	Female C57BL/6[B6], DBA/2[D2] and C3H/He[C3], 16 weeks, left tibiae	N/A	1.5(DBA, 2(C57BL/6J and C3H/HeJ)	2000	99	2	N/A	3 days/week for 3 weeks	Histomorphometry: MS/BS, MAR, BFR/BS
Krause 2020 ¹⁰⁸	Male C57BL/ J6 nice, 15 week, right tibiae	Unloading	9	1400	1200	4, sawtooth waveform	N/A	4 times per week for 6 weeks	Micro CT trabecular bone: BV/TV, Tb.N, Tb.Th, Tb.Sp, Conn.D, BMD, Cortical bone: Ct.TV, Ct.BV, Ct.BV/TV, Ct.Th, Ct.Po, Ct.BMD
Lee 2002 ¹⁰⁹	Female CD1 mice, 17 weeks, left ulnae	NA	3 and 4	2000 and 3000	NA	4	N/A	5 days/week for 2 weeks	Histomorphometry: MS/BS, MAR, BFR/BS
Lionikaite 2019 ¹¹⁰	Female C57BL/6N mice, 13 weeks, right tibiae	Vitamin A and vehicle	N/A	N/A	40	N/A	10	3 times per week for 2 weeks	Histomorphometry: MS/BS, MAR and BFR/BS, micro CT: trabecular bone: BV/TV, Tb.Th, Tb.N, Tb.Sp, cortical bone: Ct.Ar, Ct.Th, Ma.Ar periosteal and endocortical perimeter
Lynch 2010 ¹¹¹	Male & Female C57Bl/6 mice, 9 weeks, left tibia,	NA	11.5	1300	NA	4	NA	5 times per week for 2 weeks	Histomorphometry: MS/BS, MAR and BFR/BS, micro CT: BV/TV, Tb.Th, and tBMD, TbSp
Lynch 2011 ¹¹²	Female C57Bl/6 mice, 26 weeks, left tibiae	N/A	11.5 and 5.9	2100 and 1200	1200	4	N/A	5 times per week for 2 weeks	Micro CT: trabecular bone: BV/TV, cnTMD, Tb.Th, Tb.Sp, cortical bone: ct.TMD, Ct.Ar, Ma.Ar, principal moment of inertia
Meakin, 2013 ¹⁶	Male and female C57BL/6, 16 weeks, right tibiae	NA	13.3	2200	40	N/A	10	3 times per week for 2 weeks	Micro CT: trabecular bone: BV/TV, Tb.Th, Tb.Sp, Tb.N, cortical bone: Ct.Ar, T.Ar, Ma.Ar, Ct.Ar/T.Ar, Ct.Th, polar moment of inertia
Miller 2021 ¹¹³	Female C57BL/6 mice, right tibiae	neurectomy	6	N/A	40	N/A	10	2 weeks	Micro CT: cortical bone, Ct.Th
Moustafa 2012 ⁴⁷	Female C57BL/6, 19 weeks, right tibiae	NA	13.5	1800	40	N/A	10	3 days/week for 2 weeks	Histomorphometry: MS/BS, MAR, BFR/BS, micro CT: trabecular bone: Tb.BV/TV, cortical bone: Ct.BV
Norman 2015 ²¹	Female C57BL/6, 16 weeks, right ulna	NA	0.5, 1.4, 2.0, 2.6, 3.1	500, 1750, 2500, 3250, 4000	60	2	N/A	3 days/week for 2 weeks	Histomorphometry: MS/BS, MAR, BFR/BS
Park 2019 ¹¹⁴	Female C57BL/6J mice, right tibiae	Vehicle, aspirin, naproxen	3	3000	100	2, sinusoidal waveform	N/A	2 weeks	Histomorphometry: MS/BS, MAR, BFR/BS, trabecular bone: BV, BMD, cortical bone: Ct.Th, T.Ar, Ct.Ar, Ma.Ar
Roberts 2020 ¹¹⁵	Female C57BL/6 mice, 13 weeks	OVX, PTH	12	N/A	40	Trapezoid waveform	10	3 times per week for 2 weeks	Micro CT: trabecular bone: Tb. BV/TV, Tb.Th, Tb.Sp, Tb.N, cortical bone: T.Ar, Ct.Ar, Ct.Ar/T.Ar, Ct.Th, moment of inertia and eccentricity

Table 2. (Cont. from previous page).

Author/Year	Animals/age/ loaded bone	Interventions	Peak loads (N)	Strain ($\mu\epsilon$)	loading cycles (per day)	Frequency (Hz)/waveform	Rest periods (seconds)	Duration of loading experiment (days or week)	Outcomes
Robling 2002 ⁷⁰	Female C3/He, C57BL/6 and DBA/2, 20 weeks, right ulna	NA	C3H/He (2.20, 2.75 & 3.30), C57BL/6(1.85, 2.30, 2.75), DBA/2(1.55, 1.90, 2.25)	C3H/He:2392, C57BL/6:1769, DBA/2:1860	60	2	N/A	3 days	Histomorphometry: MS/BS, MAR, BFR/BS, fluorochrome histomorphometry: T.Ar, Ct.Ar, maximum second moment of inertia
Sugiyama 2010 ⁶³	Female C57BL/6, 19 weeks, right tibiae	NA	11.5	1400	40	N/A	10	2 weeks	Micro CT: Ct.BV, BV/TV, Tb.N, and Tb.Th
Warden, 2004 ⁵⁷	Female C57BL/6, 8-12 weeks, right ulna	NA	1.5 or 2	1750 or 2566	120	1, 5, 10, 20 and 30	N/A	3 days	Histomorphometry: MS/BS, MAR, BFR/BS, and micro CT: Ct.Ar, moment of inertia (I_{max} , I_{min})
Weatherholt 2013 ¹¹⁶	Female C57BL/6, 16 weeks, right tibiae	NA	7 and 9	1833	360	2	N/A	3 days/week for 4 consecutive weeks	Histomorphometry: MS/BS, MAR, BFR/BS, <i>in vivo</i> pQCT: cortical bone: BMC, T.Ar, Ct.Ar., Ma.Ar, micro CT: BV/TV, Tb.N, Tb.Th and Tb.Sp
Birkhold 2016 ⁵³	Female C57Bl/6J, 26 weeks, left tibiae	NA	11	1200	216	4	N/A	5 days/week for 2 weeks	Histomorphometry: MS/BS, newly mineralized bone volume (MV/BV), mineralization thickness (M.Th), micro CT: cortical bone; Ct.BV, Ct.Th, Ct.Ar
Zhao 2014 ²³	Male C57BL/6, right tibiae	NA	7	N/A	200	1-17 (low), 18-34 (medium), 35-51 (high frequency)	N/A	N/A	Histomorphometry: MS/BS, MAR, BFR/BS, and micro CT
Sun 2018 ⁵²	Female C57BL/6, 12 weeks, right tibiae	NA	4.2, -5.5, -7 and -8	1000, 1,400, 1,800 and 2,200	60, 300 or 1200	4	N/A	5 times or 3 times per week for 2 weeks	Histomorphometry: MS/BS, MAR, BFR/BS
Castillo 2006 ¹¹⁷	Female C57BL/6, 12 weeks, right ulna	NA	2	N/A	60	2	N/A	3 times/week for 4 weeks	Histomorphometry: MS/BS, MAR, BFR/BS
Yang 2017 ⁶⁹	C57BL/6, left tibia	NA	9	N/A	36, 216, 1200	NA	10 (between 4 cycles)		Micro CT: Ct.Ar, Ct.Th, TMD
Galea 2015 ⁶⁴	Female C57B/6J, 17-19 weeks, right tibia	OVX, aging	13.5	1250	40	N/A	N/A	3 times a week for 2 weeks	Micro CT: Ct.Ar, Ct.Th and Tt.Ar
Li 2013 ²²	Female KM mice, 8 weeks, right tibia	OVX and SHAM	N/A	1000-3000	N/A	15	N/A	3 times a weeks for 4 weeks	Micro CT: B.Ar/T.Ar, Tb.Th, Tb.Sp, Tb.N , Tb.Th, Tb.Sp
Warden 2014 ⁹²	Female C57BL/6J, 16 weeks, right tibia	OVX & SHAM, aging	9	1833	360	2	N/A	3 times a weeks for 4 weeks	Histomorphometry: MS/BS, MAR, BFR/BS, micro CT: cortical bone; BMC, Ct.Ar and Ct.Th, trabecular bone;BV/TV, Tb.Th, and Tb.N and Tb.Sp
Fritton 2008 ⁶⁵	Male C57BL/6J, 10 months, left tibia	ORX, SHAM	4.6	1200	N/A	N/A	0.1 every 4 cycles	N/A	Histomorphometry: MS/BS, MAR, BFR/BS. micro CT BV/T, Tb.Th , Tb.Sp, Tb.N and BMC
Aido 2015 ⁷¹	Female C57Bl/6J mice, 10, 26 and 78 weeks, left tibia	Aging	9 or 11	1200	216	4	N/A	5 days/week for 4 weeks	Histomorphometry: MS/BS, MAR, BFR/BS

Table 2. (Cont. from previous page).

Author/Year	Animals/age/ loaded bone	Interventions	Peak loads (N)	Strain ($\mu\epsilon$)	loading cycles (per day)	Frequency (Hz)/waveform	Rest periods (seconds)	Duration of loading experiment (days or week)	Outcomes
Birkhold 2014 ⁹³	Female C57BL/6 mice, 10, 26 and 78 weeks, left tibia	Aging	9	1200	216	4	N/A	5days/week for 4 weeks.	Histomorphometry: MS/BS, MAR, BFR/BS, micro CT: Ct.BV
Brodth 2010 ¹¹⁸	Male BALB/c mice, 28 or 84 weeks, right tibiae	Aging	8, 10 or 12	900, 1290 or 1670	60	N/A	N/A	5 days	Histomorphometry: MS/BS, MAR, BFR/BS, micro CT: trabecular bone, BV/TV, Tb.N, Tb.Th, vBMD, cortical bone: M.Ar, B.Ar, Ct.Wi
Checa 2015 ⁷⁴	Female C57B1/6J, 10 and 26 weeks, left tibia	Aging	11	1200	216	4	N/A	5 days/week for 2 weeks	histomorphometry: MS/BS, MAR, BFR/BS
De Souza 2005 ⁶⁶	Female C57BL/J6, 8, 12, 20 weeks, right tibia	Aging	2-13	500-3000	40	2	10	3 times/ week 2 weeks.	Histomorphometry: endosteal inter-label area, periosteal inter-label area, total inter-label area, micro CT: trabecular bone, BV/TV, Tb.N, Tb.Th, Tb.Sp and SMI
Holguin 2014 ⁶⁷	Female C57BL/6J mice, 20, 48 and 88 weeks, right tibia	Aging	N/A	2000-3000	1200	4	0.1	5 days/week for 2 weeks	Histomorphometry: MS/BS, MAR and BFR/BS, <i>in vivo</i> μ CT: vBMD
Main 2014 ¹¹⁹	Female C57Bl/6 mice, 6, 10 and 16 weeks, left tibia	Aging	8.8 or 9.1	1200	1200	4	NA	5 days/week for 2 weeks	Micro CT: trabecular bone, Tb. BV/TV, Tb.Th, cntMD, and Tb.Sp, cortical bone, Ct.Ar
Meakin 2014 ⁶⁸	Male and Female C57BL/6, 16 and 19 weeks, right tibiae	Aging	5-17	500-2500	40	N/A	10	3 days/week for 2 weeks	Micro CT: trabecular bone, Tb.Th, cortical bone, Ct.Ar, T.Ar, Ct.Th
Silva 2012 ¹²⁰	Female BALB/cBy, 8, 16, 28, 48 weeks, right tibiae	Aging	7.5-11	1300 or 2350	60	N/A	10	3 days per week, for 6 weeks	Histomorphometry, MS/BS, MAR, BFR/BS, micro CT, Ct.BV, BV/TV
Willie 2013 ⁷²	Female C57BL/6J, 10 and 26 weeks, left tibiae	Aging	10, 26	1200	216	N/A	5 (every 4 cycles)	5 days per week for 2 weeks.	Histomorphometry: MS/BS, MAR, BFR/BS, micro CT: BV/TV, Tb.Th
De Souza 2005 ³²	Female C57BL/J6, 10 and 20 weeks, right tibiae	Aging, sciatic neurectomy	12	2000	40	2	N/A	3 days/week for 2 weeks	Histomorphometry: MS/BS, MAR, BFR/BS
Meakin 2015 ²¹	Female C57BL/6 mice, 17 and 76 weeks, right tibiae	aging, sciatic neurectomy, sham	13 or 13.3 N	500-2500	40	N/A	10	8 loading sessions on alternate days	Histomorphometry: MS/BS, MAR, BFR/BS, micro CT: Tt.Ar, Ct.Ar, Ma.Ar
De Souza 2017 ⁷⁷	Female C57BL/J6, 8, 14, 20 and 72 weeks, right tibiae	Aging, sciatic neurectomy (5 days and 100 days period)	2-13	2000	40	2	10	six alternate days for 2 weeks	Histomorphometry: MS/BS, MAR, BFR/BS, micro CT: T.Ar, Ct.Ar, trabecular bone, BV/TV, Tb.N, Tb.Th, Tb.Sp and SMI
Shirazi-Fard 2015 ²²	Male C57BL/6J mice, 16 weeks, right tibiae	Total body irradiation with high LET iron ions	9	N/A	60	N/A	9.75	3 day/week for 4 weeks	Histomorphometry: MS/BS, MAR, BFR/BS, micro CT: trabecular bone, BV/TV, Tb.Th, Conn.D, TMD, cortical bone: Ct.Th, CSA and Ct.BV

Table 2. (Cont. from previous page).

Author/Year	Animals/age/ loaded bone	Interventions	Peak loads (N)	Strain ($\mu\epsilon$)	loading cycles (per day)	Frequency (Hz)/waveform	Rest periods (seconds)	Duration of loading experiment (days or week)	Outcomes
Sugiyama, 2012 ¹²³	Female C67BL/6, 17 weeks, right tibiae	Right sciatic neurectomy	14	5000	40	N/A	10	on alternate days for 2 weeks	Micro CT: BV/TV
Rapp 2015 ¹²⁴	C57BL/6J, 18 weeks, right ulna	Mesenchymal stem cell or vehicle	1.5	N/A	N/A	2	N/A	5 times a week for 2 weeks	Histomorphometry: MS/BS, MAR, BFR/BS, micro CT: Ct.BV
Leucht 2013 ⁵⁰	C57BL/6 mice, SRXG mice, 16 weeks, right ulna	AMD3100 (CXCR4 receptor antagonist) & vehicle	2.8	3550	120	2	N/A	N/A	Histomorphometry: MS/BS, MAR, BFR/BS
Marenzana 2007 ¹²⁵	Female C57Bl/J6 mice, 9 weeks, right tibia	β -adrenergic antagonist (Propranolol) & vehicle	12.5	1500	40	N/A	10	3 alternate days per week for 2 weeks	Micro CT: trabecular bone;Tb.BV/TV and Tb.Th, cortical thickness: Ct.Th, B.Ar, T.Ar and Ma.Ar
McAteer 2010 ¹²⁶	Female C57BL/6J mice, 10 weeks, right ulna	Low dose PTH, high dose PTH, vehicle	1.95 or 2.25	1800-2200	N/A	2	N/A	3 days	Histomorphometry: MS/BS, MAR, BFR/BS, DXA: aBMD and BMC
Moustafa 2009 ¹²⁷	Female C57BL/6 mice, 19 weeks, right tibiae	iPTH & vehicle	13.5	1400	N/A	N/A	N/A	3 alternate days per week for 2 weeks	Histomorphometry: MS/BS, MAR, BFR/BS, micro CT: Ct.BV
Sugiyama, 2008 ³⁰	Female C57BL/6, 7 weeks, right tibiae and ulna	human iPTH low, medium or high dose & vehicle	2.5 (ulna), 12 (tibia)	1200 (tibia), 1350 (ulna)	40	N/A	10	3 days /week for 2 weeks.	Histomorphometry: MS/BS, MAR, BFR/BS, micro CT: trabecular bone, BV/TV, Tb.N and Tb.Th, cortical bone, Ct.BV
Sugiyama, 2013 ⁸⁵	Female C57BL/6, 19 weeks, right tibiae	COX-2 inhibitor (NS-398) & vehicle	13.5	1800	40	N/A	10	3 days /week for 2 weeks	Micro CT: trabecular bone; BV/TV, Tb.Th, Tb.N, cortical bone; Ct.BV
Stadelmann 2011 ¹²⁸	Male C57BL/6, 17 weeks, left tibiae	Bisphosphonate (zoledronate) treatment & saline	8	1800 at postero-tibial crest 1940 at anterodistal tibia	N/A	2	N/A	on day 1, 3, 5, 8 and 10	<i>In vivo</i> micro CT: B.Pm, B.Ar, Ct.Th
Sugiyama, 2010 ²⁸	Female C57BL/6, 17 weeks, right tibiae	OVX & SHAM, tamoxifen low, medium, high & vehicle	10	1200	40	N/A	10	3 days/week for 2 weeks	Micro CT: trabecular bone; BV/TV, Tb.Th, cortical bone; Ct. BV
Sugiyama, 2011 ²⁹	Female C57BL/6, 17 weeks, right tibia	Bisphosphonate (residronate) treatment & vehicle	11.5	1200	40	N/A	10	3 days/week for 2 weeks	Micro CT: trabecular bone BV/TV, Tb.Th and cortical bone: Ct.BV
Borg 2018 ¹²⁹	Female C57BL/6, 10 and 18 weeks, left tibiae	Vitamin D supplemented diet or vitamin D free diet	10.5	N/A	40	N/A	10	3 times per week for 2 weeks	Histomorphometry: MS/BS, MAR, BFR/BS, micro CT: trabecular bone: TV, BV, BV/TV, cortical bone: Ct.Th, Ct.Po

Table 2. (Cont. from previous page).

Author/Year	Animals/age/ loaded bone	Interventions	Peak loads (N)	Strain ($\mu\epsilon$)	loading cycles (per day)	Frequency (Hz)/waveform	Rest periods (seconds)	Duration of loading experiment (days or week)	Outcomes
Govey 2016 ¹³⁰	Female C57BL/6J, 16 weeks, right tibiae	Total body irradiation (67.5 CgY/min), bone marrow transplantation	10	N/A	1200	4	N/A	5 days per week for 3 weeks	Micro CT: trabecular bone; BV/TV, Tb.Th, ConnD, Cortical bone; Ma.Ar, Ct.Ar/T.Ar, Ct.Th, Ct.BMD, TMD
Meakin 2017 ¹³¹	Female C57BL/6, 76 weeks, right tibiae	Aging, PTH treatment	12.6	N/A	40	N/A	N/A	3 times per week for 6 weeks	Histomorphometry: MS/BS, MAR, BFR/BS, micro CT: trabecular bone: BV/TV, cortical bone: Ct.Ar and T.Ar, Ct.Th
Heffner 2017 ¹³²	Female C57BL/6	Neonatal capsaicin and vehicle treatment	3 and 7	N/A	1200	N/A	N/A	5 days/week for 2 weeks	Histomorphometry: MS/BS, MAR, BFR/BS, micro CT: cortical bone, T.Ar, BMC
Wang 2018 ¹³³	Female ICR mice, 8 weeks,	OVX- icarine vehicle,	N/A	2500	N/A	15	N/A	3 times per week for 4 weeks	Micro CT: trabecular bone, BV/TV, BMD, Tb.Th, Tb.N, Tb.Sp, Tb.Pf
Wang 2021 ¹³⁴	Female C57BL/6J	N/A	4.5 or 8	N/A	300	4	N/A	5 days per week for 4 weeks	Trabecular bone:Tb.BV/TV, Tb.Th, Tb.Sp, Tb.BMD, Tb.TMD. cortical bone:Ct.BMD, Ct.TMD, polar moment of inertia
Yang 2021 ¹³⁵	Female C57BL/6 mice, 15 weeks, left tibia	N/A	3.5, 5.2 or 7.5	694, 1034 or 1389	216	4	5	3 days or 10 days session over 2 weeks	Cortical bone: Ct.Ar, T.Ar, Ma.Ar, Ct.Th, moment of inertia, trabecular bone: BV/TV, Tb.Th, Tb.Sp, histomorphometry: MS/BS, MAR, BFR/BS
Lu 2019 ¹³⁶	C57BL6/J mice, 8 and 16 weeks,	N/A	10.5	N/A	40	Trapezoid waveform	N/A	3 times per week for 2 weeks	Trabecular bone: BV.TV, Tb.N, Tb.Sp, Tb.Th, cortical bone: Ct.Th, Ma.Ar
Zouti 2019 ¹³⁷	BALB/c mice, 10 weeks, right tibia	N/A	10	2000	216	4	5 (every 4 cycles)	5 days per week for 3 weeks	Cortical bone: Ct.Ar, Ct.At/T.Ar, Ct.Th, Ct.vTMD, PoV, Ct. Po, trabecular bone: BV/TV, Tb.Th, Tb.N, Tb.Sp, Tb.vTMD, histomorphometry: MS/BS, MAR, BFR/BS
Javaheri 2020 ¹³⁸	Female C57BL/J6 mice, 12 weeks,	N/A	12	N/A	40	2	10	3 days per week for 2 weeks	Cortical bone: cross-sectional area, cortical thickness, histomorphometry: MAR

summarized in Tables 2 and 3. Peak load ranged from 1.5 to 3.5 N in mouse ulna and from 1 to 17 N in mouse tibia studies. In most mice studies, strain gauge was used to calculate strain magnitudes. Strain magnitudes ranged from 500 to 4000 $\mu\epsilon$ in mouse ulna studies, and 500 to 5081 $\mu\epsilon$ in mouse tibia studies. Two studies used micro CT derived simulated strain measurement at the mid-shaft^{21,22}; this technique allows the estimation of strain in proximal, medial, and distal sites of the tibia, without the need for strain gauge attachment at the bone sites and eliminates the sacrifice of the animals for this process^{21,22}. The computational method of strain determination provides a suitable alternative to strain gauge, as it provides more accurate measurement of peak strain and eliminates the large variability of strain due

to placement of strain gauge in small curved mouse bones²¹. Frequency and number of cycles in mouse ulna studies ranged from 2 to 15 Hz and 40 to 9000 cycles per day, while in mouse tibia studies it ranged from 1 to 51 Hz and from 40 to 1200 cycles per day. Mouse axial loading studies generally used loading sessions that were repeated five times a week for one week up to six weeks^{16,19,47-49}, and only two mouse studies reported a single loading session^{50,51}. One mouse axial loading study reported that a loading session of five days per week for two weeks showed a better response in bone formation as compared to a three alternate days per week loading for two weeks⁵². The loading session of five consecutive days showed a larger increase in MS/BS (+38%) as compared to a three days per week loading session, which showed only

15% increase in periosteal MS/BS⁵². Moreover, there was no difference in bone formation between the loading session of five days per week for one week or five days per week for two weeks. The periosteal MS/BS increased 42.2% in one week and 38.1% in two weeks⁵². In the same study, no differences in MS/BS were observed in between three loading cycles of 60, 300 and 1200 when a 1800 $\mu\epsilon$ strain was applied⁵².

Mechanical loading increased BV/TV, Tb.Th, tissue mineral density (TMD) in trabecular bone, cortical area, and cortical thickness in cortical bone. These effects became more pronounced with an increase in strain levels of 1700 $\mu\epsilon$ (low), 2050 $\mu\epsilon$ (medium) and 2400 $\mu\epsilon$ (high)⁴⁸. While loading at a strain level of 2050 $\mu\epsilon$ (compressive force 10.6 N) caused a strong formation response, a lower strain of 1700 $\mu\epsilon$ (compressive force 8.8 N) had a smaller effect, and a higher strain of 2400 $\mu\epsilon$ (compressive force 12.4 N) caused rapid bone formation, but led to the formation of woven bone in half of the animals. This suggests that the effective strain window for bone formation may be rather small⁴⁸. Mechanical loading significantly increased the bone formation parameters, increasing newly mineralized volume by 134% and mineralizing surface by 50%. It decreased the bone resorption parameters (resorbed bone volume and eroded surface) at the metaphyseal periosteal region of bone, while diaphyseal remodeling was more pronounced at the endosteal surface. Setpoints and slopes for strain-mediated responses were different for the endosteal and periosteal surfaces in the metaphyseal and diaphyseal regions, suggesting that the bone formation response is site and region specific⁵³. In KO mouse models, separate measurements of strain were performed with a strain gauge in both KO mice and controls⁵⁴⁻⁵⁶. In Connexin 43 deficient mice, peak loads of 3.1 N and 3.5 N increased MAR, MS/BS, and BFR/BS, but 2.8 N did not⁵⁵. A mouse study that applied 1.6 N at different frequencies of 1, 5, 10, 20, or 30 Hz, reported significant influence of loading frequency in cortical bone geometry. Loading at 5 Hz frequency showed significantly greater changes in cortical area (Ct.Ar) as compared with either 1 or 20 Hz, loading at 30 Hz resulted in significantly greater Ct.Ar than 1 Hz, but no other statistical differences were reported among the frequencies⁵⁷. In their short term loading experiment for 3 consecutive days, a load of 2.0 N increased rMAR, rMS/BS and rBFR/BS with a frequency of 10 Hz as compared to frequencies of 1, 2, and 5 Hz, but there were no differences in rBFR/BS between 10 and 30 Hz, as the cortical bone adaptation plateaued out above frequencies of 10 Hz⁵⁷. Similarly, their long-term loading experiment for 4 weeks with a peak load of 1.6 N showed that cortical bone adaptation increased with loading of 5-10 Hz and plateaued out beyond frequencies of 10 Hz⁵⁷.

Rest periods between loading cycles were used in thirty-five mouse studies^{16,28,47,49,54,58-68}, but none of them were compared with a non-rest period control^{16,28,47,49}. In one of these studies, a loading protocol of peak load 10 N, 60 loading cycles, 2 Hz frequency, and 10s rest period, 3 days a week for 6 weeks, was compared with a loading protocol of peak load 10 N, 1200 loading cycles, 6.7 Hz frequency and 0.1s

rest period, which could be considered no rest, 3 days a week for 6 weeks⁴⁹. The loading protocol with 0.1s rest actually showed a more rapid and greater response in bone formation than the protocol with 10s rest after the first three weeks of loading. However, after six weeks, similar bone formation was reported in the two loading protocols⁴⁹. Another study compared 10s rest inserted after 4 cycles each for 216 cycles compared with 216 continuous cycles with no rest period using 9.0 N peak load and 4 Hz frequency in both groups and found similar increases in cortical bone parameters (cortical area (Ct.Ar), cortical thickness (Ct.Th), Total cross-sectional area (Tt.Ar), marrow area (MaAr) and maximum moment of inertia (I_{max})) and metaphyseal cancellous bone parameters (BV/TV, Tv.Th and tissue mineral density (TMD))⁶⁹. Addition of a rest period between cycles was not beneficial in improving bone outcomes in their study as compared to a continuous loading session with no rest period⁶⁹.

Axial loading was mostly carried out in female C57BL/6 mice^{19,21,28,47,49} though strain specific responses in bone formation were observed for C3H/He, C57BL/6 and DBA/2 mice⁷⁰. Aged mice were less responsive to load-induced periosteal bone formation, measured as MS/BS, MAR and BFR/BS⁷¹⁻⁷⁴, as compared to young mice, and aged mice showed diminished microstructural changes in both trabecular⁷¹⁻⁷³ and cortical regions^{50,54,73,75} of bone, as compared to young mice. OVX mice showed deteriorated B.Ar/T.Ar, Tb.Th and increased Tb.Sp as compared to SHAM but loading increased B.Ar/T.Ar and Tb.Th, but decreased Tb.Sp in loaded OVX mice as compared to non-loaded OVX mice²². Tamoxifen treatment in the loaded OVX mice increased BV/TV, Tb.Th, Ct.BV, and periosteally-enclosed volume, as compared to vehicle-receiving sham and OVX groups, indicating a positive effect of tamoxifen in loading-related gain in both trabecular and cortical bone mass²⁸. In orchietomized mice (ORX), mechanical loading did not prevent cancellous bone loss associated with ORX⁶⁵. Disuse induced by sciatic neurectomy resulted cortical bone loss in mice³². Axial loading increased cortical bone formation restoring the bone loss in mice immobilized by sciatic neurectomy for 4⁷⁶, 5^{32,77} or 100 days⁷⁷. Similarly, loading significantly increased cortical bone formation in mice immobilized by neurectomy for 5 days as compared to SHAM controls in both growing and adult mice. One study in 19 months old mice reported that prior and concurrent sciatic neurectomy significantly enlarged loading-induced increases in cortical bone total cross-sectional area (T.Ar) and trabecular bone thickness (Tb.Th), and structural model index (SMI). Mechanical loading after prior and current disuse resulted in site-specific rescue of age-related loss of mechanoresponsiveness. This occurred mainly in the 20% of cortical bone sites where there was greatest age-related decline in responsiveness⁷⁸. One recent study in mice reported that the time of day at which loading was administered influenced the bone formation in a site-specific manner⁷⁹. Mice loaded at 8:00 pm showed more cortical bone formation response: newly mineralized volume fraction (MV/BV), mineralizing bone surface (MS/BS), and mineralizing thickness (MTh) at the endocortical surface

Table 3. Summary of knock out mouse axial loading studies.

Author/Year	Mice studies	Interventions	Peak load (N)	Strain ($\mu\epsilon$)	loading cycles (per day)	Frequency (Hz)/waveform	Rest periods (seconds)	Duration of loading experiment (days or week)	Loading induced outcomes in bone
Alam 2005 ¹³⁹	Female COX-2 ^{-/-} , COX-2 ^{-/-} , 16 weeks, right ulna	NA	2.1	2580	120	2	N/A	2 days	Histomorphometry: MS/BS, MAR, BFR/BS, micro CT
Bivi 2013 ⁵⁵	Female CX43 ^{Δot} , CX43 ^{fl/fl} , 17 weeks, right ulnae	NA	2.3, 2.5 and 2.8 (CX43 ^{fl/fl} mice), 2.8, 3.1 and 3.5 (CX43 ^{Δot} mice)	N/A	120	N/A	N/A	3 days	Histomorphometry: MS/BS, MAR, BFR/BS
Bonnet 2009 ⁵⁸	Postn ^{-/-} , Postn ^{+/-} , and Postn ^{-/-} , 14 weeks, left tibiae	NA	12	1500	40	0.1	10	3 days/week for 2 weeks	Micro CT: BV/TV, Tb.N, Tb.Th, TV, Ct. BV, Ct.Th, Histomorphometry: MS/BS, MAR, BFR/BS
Callewaert 2010 ⁵⁹	Male AR-ERα KO, ERα KO, AR KO, and WT, and female WT, ERα KO, 20-22 weeks, left ulnae	NA	2.5	1560-1740	40	N/A	14.9	3 alternate days for 2 weeks	Histomorphometry: MS/BS, MAR, BFR/BS
Castillo 2012 ¹⁴⁰	Male and female FAK-KO and WT, 16 weeks, right ulnae	NA	3.0 (males), 2.8 (females)	3500	60	2	N/A	3 days	Histomorphometry: MS/BS, MAR, BFR/BS, micro CT: trabecular bone, BV/TV, Tb.N, Tb.Th, Tb.Sp, ConnD, SMI, cortical bone, Ct.Ar, Ct.Th
Grimston 2012 ⁵⁴	WT and cKO (DM1Cre; ^{Gja1} ^{fllox/2}), 8 weeks, right tibia	NA	8	1200	60	N/A	10	5 days	Histomorphometry: MS/BS, MAR, BFR/BS, micro CT: Ct.BV, M.Ar, T.Ar
Javaheri 2014 ¹⁴¹	Male and female HET cKO & WT, 18-24 weeks, right ulna	NA	18-24	2500	100	2	N/A	3 days/week for 3 weeks	Histomorphometry: MS/BS, MAR, BFR/BS, micro CT: trabecular bone: BV/TV, Tb.Th, BMD, cortical bone: Ct.BMD, Ct.Th
Kesavan 2011 ⁶⁰	Female IGF-I KO and WT, 6 weeks, right tibiae	NA	6-12 (female), 6.5-12 (male)	745 and 780	40	N/A	10	3 days/week for 2 weeks	Micro CT: trabecular bone; Tb.BV/TV, Tb.BMD, cortical bone; Ct.TV, TMD, and Ct.Th
Lee 2004 ⁸²	ERα ^{-/-} & ERβ ^{-/-} and ERα ^{+/-} and ERβ ^{+/-} mice, 20-24 weeks, left ulnae	NA	3.4	2800	40	N/A	14.9	3 alternate days each week for 2 weeks	Histomorphometry: MS/BS, MAR, BFR/BS, micro CT:Ct.Ar
Liedert 2011 ¹⁴²	Mdk-deficient mice and WT, 51-52 weeks, right ulnae	NA	2.5	1825-1920	120	2	N/A	5 consecutive days for 2 weeks	Histomorphometry: MS/BS, MAR, BFR/BS, micro CT: cortical bone, Ct.Th, T.Ar, Ma.Ar, Ct.Ar, moment of inertia I _{min} and I _{max}
Litzenberger 2009 ¹⁴³	Female Coll(α1) cKO and WT, 16 weeks, right ulna	NA	3	3000	120	2	N/A	3 consecutive days	Histomorphometry: MS/BS, MAR, and BFR/BS, <i>in vivo</i> micro CT: trabecular bone, BV/TV, Tb.N, Tb.Sp, Tb.Th, ConnD, cortical bone, T.Ar, minimum and maximum moment of inertia (I _{min} and I _{max})
Melville 2015 ⁸¹	Male and female pOC-ERαKO mice and Littermate control (LC), 10 weeks, left tibiae	NA	9.0	1200	1200	4	N/A	5 days per week for 2 weeks	Histomorphometry: MS/BS, MAR, and BFR/BS, micro CT: BV/TV, Tb.Th, Ct.Ar
Morse 2014 ¹⁴⁴	Female Sost ^{-/-} and WT, 10 weeks, left tibia	NA	9 or 12.5	1200	1200	N/A	N/A	5 days/week for 2 weeks	Histomorphometry: MS/BS, MAR, and BFR/BS, micro CT: BV/TV, DXA: BMD
Niziolek 2012 ¹⁴⁵	Male LRP5 (G171V & A214V) and WT, 18 weeks, right tibia	NA	9, 9.8 and 14.4	2120	120	2	N/A	3 bouts at alternate days	Histomorphometry: MS/BS, MAR, and BFR/BS
Parajuli 2015 ⁵⁶	Male and female heterozygous C57BL/6-Ins2 ^{Akita} /J (Akita), 28 weeks, right ulna	NA	2.7 N Akita females, 2.2 N Akita males	3500	N/A	2	N/A	5 consecutive days	Histomorphometry: MS/BS, MAR, and BFR/BS, micro CT: Ct.T.Ar, Ct.B.Ar and Ct.Th
Pierroz 2012 ¹⁴⁶	Adrb1 ^{-/-} , Adrb2 ^{-/-} and WT, 16 weeks, left tibiae	NA	12	1500	40	0.1	N/A	3 days/week for 2 weeks	Histomorphometry: MS/BS, MAR, and BFR/BS, micro CT: Tb.BV/TV and Ct.BV, Ct.Th, DXA: BMD

Table 3. (Cont. from previous page).

Author/Year	Mice studies	Interventions	Peak load (N)	Strain ($\mu\epsilon$)	loading cycles (per day)	Frequency (Hz)/waveform	Rest periods (seconds)	Duration of loading experiment (days or week)	Loading induced outcomes in bone
Robling 2007 ¹⁴⁷	Male and female B6C3H-1T(1T), B6.C3H-8T (8T), B6.C3GH-13B, C57BL/6J, 13 weeks, right ulna	NA	N/A	N/A	60	2	NA	3 consecutive days	Histomorphometry: MS/BS, MAR, and BFR/BS
Saxon 2007 ⁷⁵	Male and female, ER- $\beta^{+/+}$, ER- $\beta^{+/-}$, ER- $\beta^{-/-}$, 16 weeks, right ulna	NA	N/A	1400	N/A	2	NA	Daily for 3 consecutive days	Histomorphometry: MS/BS, MAR, and BFR/BS, DXA: BMD, BMC, pQCT : BMC, B.Ar, vBMD
Sinnesael 2012 ⁶¹	Male AR(ocy-ARKO), WT, 18 weeks, right tibia	NA	16.5	N/A	40	N/A	10	3 times a week for 2 weeks	Histomorphometry: MS/BS, MAR, and BFR/BS, micro CT, DEXA: BMD
Tomlinson 2015 ¹⁴⁸	Female Δ HIF-1 α mice and WT, 18-22 weeks, right ulna	NA	3.5	N/A	100	2	N/A	NA	Histomorphometry: MS/BS, MAR, and BFR/BS
Tu 2012 ⁸⁶	Female hemizygous Dmp1-Sost transgenic mice and WT, 4, 8 and 16 weeks, right ulna	NA	1.90 (low), 2.20, (medium) and 2.50 (high)	2460, 2850, 3240	120	N/A	N/A	3 consecutive days	Histomorphometry: MS/BS, MAR, and BFR/BS
Wang 2013 ¹⁴⁹	P2Y ₁₃ R ^{-/-} and WT, 16 weeks, left tibia	NA	14.5	5048	40	N/A	10	3 times a week for 2 weeks	Histomorphometry: MS/BS, MAR, and BFR/BS, micro CT: trabecular bone, BV/TV, Tb.Th, Tb.N, cortical bone, Ct.BV
Zhao 2013 ¹⁵⁰	Dmp1-Cre;Lrp1 ^{+/+} (cKO) and WT, 13 weeks, right ulna	NA	2.65	N/A	360	2	N/A	3 consecutive days.	Histomorphometry: MS/BS, MAR, BFR/BS, pQCT: BMC, vBMD, DXA: BMD
Svensson 2016 ¹⁵¹	IGF-I KO mice and Controls, 24 and 76 weeks, right tibiae	NA	11 and 13.5	3500 and 2800	40	N/A	10	3 times per week for 2 weeks	Micro CT: BV/TV
Tomlinson 2017 ⁸⁷	TrKA ^{F592A} mice, Thy1-YFP mice, 16-20 weeks, right ulna	NA	3	N/A	100	0.1	N/A	3 days	Histomorphometry: MS/BS, MAR, and BFR/BS
Xiao 2011 ¹⁵²	Dmp1-Cre;Pkd1 ^{fllox/miBei} , Pkd1 ^{fllox/miBei} and Dmp1-Cre; Pkd1 ^{fllox/+} , 16 weeks, right ulna	NA	3	N/A	180	2	N/A	3 days per week for 3 weeks	Histomorphometry: MS/BS, MAR, and BFR/BS
Lories 2007 ¹⁵³	Frzb ^{-/-} mice and WT, 17 weeks, left ulna	NA	4	N/A	N/A	4	N/A	10	pQCT: Ct.BMC, Ct.BMD, Ct.Th
Mohan 2014 ¹⁵⁴	female IGF-I KO or WT, 10 weeks, right tibiae	OVX & SHAM	10	745 and 780	40	N/A	10	3 alternate days/week for 2 weeks	Micro CT: TV, BV/TV, Ct.Th, BMD, Tb.N, Tb.Th, Tb.Sp
Windahl 2013 ⁸⁰	Female ER $\alpha^{-/-}$, ER α AF-1 $^{\circ}$, ER α AF-2 $^{\circ}$ and WT(sham ovx), 17 weeks, right tibiae	OVX & SHAM	6-14	3050	40	N/A	10	3 alternate days per week for 2 weeks	Histomorphometry: MS/BS, MAR, and BFR/BS, micro CT:Tb.BV/TV, BMD, Tb.N, Tb.Th, pQCT: BMD, Ct.Ar
Saxon 2011 ¹⁵⁵	Male and female Lrp5 ^{-/-} mice, Lrp5 ^{HBM+} mice and WT, 17 weeks, right tibia	Sciatic neurectomy	N/A	1500, 2400 and 3000	40	N/A	14.9	3 alternate days per week for 2 weeks	Micro CT : BV/TV, Tb.Th, Ct.Ar, T.Ar, Ma.Ar
Kang 2016 ⁵¹	Male, β Cat ^{+/+} , Dmp1-CreERT2- or CreERT2+& WT, 18 weeks, right ulna	Tamoxifen or oil	2.85	2740-2980	180	2	N/A		Histomorphometry: MS/BS, MAR or BFR/BS, DEXA: BMD
Pflanz 2017 ¹⁵⁶	Sost KO and LC mice, 10 and 26 weeks, left tibiae	Aging	N/A	900	216	N/A	0.1 (between cycles), 5 (every four cycles)	5 days/week for 2 weeks	Histomorphometry: MS/BS, MAR or BFR/BS

Table 3. (Cont. from previous page).

Author/Year	Mice studies	Interventions	Peak load (N)	Strain ($\mu\epsilon$)	loading cycles (per day)	Frequency (Hz)/waveform	Rest periods (seconds)	Duration of loading experiment (days or week)	Loading induced outcomes in bone
Moore 2018 ¹⁵⁷	Prx1CreER-GFP; ROSA26 ^{DTA} mutant and ROSA26 ^{DTA} controls, 16 weeks, right ulna	Tamoxifen treatment	3	120	120	2	N/A	3 days	Histomorphometry: MS/BS, MAR or BFR/BS, micro CT: BV/TV, BMD, Ct.Th, the polar moment of inertia (J), and the minimum and maximum second moments of inertia (I_{min} and I_{max})
Robling 2016 ¹⁵⁸	Sost ^{-/-} mice, ECR5 ^{-/-} mice and controls, 16 weeks, right ulna	Hind limb suspension	N/A	1800, 2300 or 2800	180	2	N/A	3 days/week for 2 weeks	Histomorphometry: MS/BS, MAR or BFR/BS, micro CT: BV/TV, Tb.Th, DXA: BMC
Sawakami 2006 ¹⁵⁹	Male and female <i>Lrp5</i> ^{-/-}	PTH	N/A	N/A	60	2	N/A	3 days	Histomorphometry (calcein): MS/BS, MAR or BFR/BS micro CT: cortical bone, Ct.Ar, polar moment of inertia, trabecular bone: BV, BV/TV, Tb.N, Tb.Th, Tb.Sp, Conn.D, pQCT: BMC, DEXA: vBMD
Lee 2014 ¹⁶⁰	AC6-KO mice and WT, 16 weeks, right ulna	PTH	3	N/A	10	2	N/A	3 days	Histomorphometry: MS/BS, MAR or BFR/BS, micro CT: cortical bone, T.Ar, Ct.Ar, Ct.Th, and minimum and maximum second moments of inertia (I_{min} and I_{max}), trabecular bone, BV/TV, Conn D, Tb. N,Tb.Th, and Tb. Sp
Sample 2014 ¹⁶¹	CGRP α and CGRP β KO and WT, 19-21 weeks, right ulna	Brachial Plexus Anesthesia (BPA)	2.49	3500	800	2	N/A	3 days	Histomorphometry: MS/BS, MAR or BFR/BS, DEXA: BMD
Albiol 2020 ¹⁶²	Sost KO and LC, age, left tibia	Sost KO	N/A	900	216	4, triangular waveform	0.1 (every load cycle) and 5 (every four cycles)	5 days per week for 2 weeks	Micro CT: Tb.BV/TV, Tb.Th, Tb.V TMD and bone histomorphometry: Tb. MS/BS, Tb.MAR and Tb. BFR/BS
Davis 2019 ¹⁶³	Osx-Cre;NT3 (NT3-Cre+) mice and Cre-negative Controls 16 weeks old, right tibiae	Osx-Cre;NT3 (NT3-Cre+)	8.7 or 10	2000	1200	4, triangular waveform	0.1	9 days	Histomorphometry: MS/BS, MAR and BFR/BS
Gerbaix 2021 ¹⁶⁴	Periostin KO mice and controls, Left tibiae	Anti-sclerostin antibody (Scl-Ab) treatment and VEH	12 or 16	1500	40	trapezoid waveform	10		Micro CT: trabecular bone: BV/TV, Tb.N, Tb.Th, Tb.Sp, Conn.D and SMI, cortical bone: Ct.Th, Ct.BV, Ct.TV, TND, Ct.Po, Ma.V
Lawson 2021 ¹⁶⁵	OsxCreERT2; WisF/F experimental and WisF/F controls, 5 months old	N/A	8 or 12	2200	60	4	N/A	5 days	Histomorphometry: MS/BS, MAR and BFR/BS
Lewis 2020 ¹⁶⁶	Dmp1-Cre transgenic mice and Cre-negative mice, 16 weeks, right tibiae	N/A	8.0 – 9.4	2250	180	2	N/A	3 bouts of load on 5 days	Histomorphometry: MS/BS, MAR, BFR/BS, DEXA: BMD
Moore 2018 ¹⁵⁷	Prx1CreER-GFP; Rosa26DTA(-/+) and Rosa26DTA(-/+)	N/A	3	N/A	120	2, sine wave	N/A	3 days	Micro CT: trabecular bone volume: BV/TV, BMD, cortical bone: Ct.Th, mean polar moment of inertia, minimum and maximum second moment of inertia, histomorphometry: MS/BS, MAR, BFR/BS
Moore 2019 ¹⁶⁷	Prx1CreER-GFP; Kif3a ^{fl/c} and controls	N/A	3	N/A	120	2	N/A	3 days	Histomorphometry: MS/BS, MAR, BFR/BS

Table 3. (Cont. from previous page).

Author/Year	Mice studies	Interventions	Peak load (N)	Strain ($\mu\epsilon$)	loading cycles (per day)	Frequency (Hz)/waveform	Rest periods (seconds)	Duration of loading experiment (days or week)	Loading induced outcomes in bone
Morse 2020 ¹⁶⁸	Dkk1 KO mice, Wnt3 ^{-/-} and wild type	N/A	7 or 12	1200	N/A	N/A	N/A	5 days per week for 2 weeks	Micro CT: trabecular bone: TV, BV/TV, TMD, Tb.Th, Tb.N, Tb.Sp, cortical bone: Ct.BV, Ct.Th, TMD, polar moment of inertia, histomorphometry: MS/BS, MAR and BFR/BS
Yang 2021 ¹³⁵	Sost KO and WT, 10, 26 and 52 weeks, left tibiae	N/A	N/A	900	216	4, triangular waveform	5 (every four cycles)	5 days per week for 2 weeks	Micro CT: cortical bone: Ct.Ar, T.Ar, Ct.Ar/T.Ar, Ct.Th, Ct.TMD, histomorphometry: MS/BS, MAR, BFR/BS.
Zannit 2020 ¹⁶⁹	3.6Colla1-tk mice and controls, 5 month and 12 months, right tibiae	N/A	7 or 11	800 and 1400	1200	4, triangle waveform	0.1	5 days	Histomorphometry: MS/BS, MAR, BFR/BS
Zannit 2019 ¹⁷⁰	Male and female Osx-Cre-ERT2 ^{+/-} ; Ai9 ^{+/+} (iOsx-Ai9) and iOsx-Ai9 controls, 5 and 12 months	N/A	11 or 14	N/A	1200	4, triangle waveform	0.1	5 days	Histomorphometry: MS/BS, MAR, BFR/BS

than mice loaded at 8:00 am, but these changes were not observed in the periosteal surface. Similarly, loading induced higher increases in cortical bone: Ct.Ar/T.Ar in the mice loaded at 8:00 pm (11% increase as compared to control) as compared to mice loaded at 8:00 am (8% increase). Similarly, Ct.Th was increased and Ma.Ar was decreased in load versus control limbs in both morning and evening groups⁷⁹.

From all publications on KO mice, four articles concerned ER- α KO mice^{59,80-82}, two articles concerned ER- β KO mice^{83,84}, and two articles concerned AR-KO mice^{59,61}. These studies consistently indicated that ER- α KO mice showed reduced osteogenic responses to loading with reduced cortical bone area^{80,84} and bone formation rates^{59,80,81,84} as compared to wild type mice. Effects of drug treatment^{28,29,85}, PTH³⁰, and KO models^{81,83,86,87} on mice axial loading-related bone outcomes are also outlined in Table 4.

Discussion

This review examines the effect of methodological aspects such as peak load and strain, frequency, number of cycles, duration of the loading sessions and rest periods independently and in conjunction with modifying factors such as age, sex-steroid deficiency and disuse in axial loading protocols, on bone outcomes. Method variations in mentioned studies are large, and the rationale for the chosen methodology in studies is not always clear. Peak load and consequently strain, frequency, number of loading cycles per day and rest period mostly varied among the selected rat and

mouse axial loading studies, which was mainly due to variations in instrumental setup, loading cups, and adjustment of these methodological aspects. The effective window of strain magnitude that causes lamellar bone formation but not woven bone formation was rather small. Site-wise differences in strain were reported in proximal, medial, and lateral ulnar and tibial sites, which resulted in variation in strain at different sites of bone after axial loading. Axial loading-induced bone formation was affected by modifying factors such as age, ovariectomy and disuse. The variation in these methodological aspects and modifying factors affected bone outcomes of mass, structure, and bone mineral density.

Mechanical loading protocols and modifying factors affecting bone outcomes in rats

This review revealed that axial loading-related bone outcomes were mainly affected by load, strain, number of cycles, frequency, duration of loading sessions and possibly rest period between cycles. The load applied is usually based on strain, or strain-rate, required for bone formation. This was determined in each loading protocol using strain gauges for load-strain calibration. However, non-invasive computational methods of strain determination such as finite element analysis and digital image correlation have been reported, which detect strain on different sites of bone. These methods have shown similar or improved reproducibility in strain determination as compared to strain gauges^{18,88}. Remarkably, a change in frequency or number of cycles increased bone mineral density when peak loads were kept constant in rat studies^{9,37}. Number of cycles and frequency should be carefully adjusted in the loading protocols, as the

Table 4. Frequently used parameters and suggestions for rats and mice axial loading protocols.

Frequently used parameters/factors affecting axial loading	Frequently used in rat studies	Frequently used in mouse studies	General suggestions for axial loading protocols
Peak load	17N ulna ^{24,25,27,36,38}	13.5 N tibia ^{47,64,85,127} , 2.5 N ulna ^{30,126}	Peak loads are determined with load- strain calibration using a strain gage. However, strain gauges have some limitations, as glueing of the strain gauge on small mouse ulna is likely to alter the mechanical properties and measured strain. Alternatively, micro CT derived finite element models can be used to calculate strain.
Strain	3600µε ulna ^{24,25,38,40}	1200 µε tibia ^{28,30,65,71,93} 2000 µε ulna ^{19,126}	Site-wise determination of strain may be performed using <i>in vivo</i> micro CT and finite element analysis.
Frequency/ Number of cycles/loading waveforms	2 Hz ^{17,24,25,27,38,40,41,43} , 360 cycles/day ^{20,25,34,35,38,41,42,44}	2 Hz ^{19,32,116,158} , 40 cycles per day in tibia ^{16,28,32,47,64,85,121,125,139} , 120 cycles per day in ulna ^{86,139,142}	Frequency and number of cycles per day should be adjusted with regard to strain/peak loads. Sine, trapezoid, triangular, or haversine waveforms may be used.
Rest period	10s ³¹	10s ^{16,28,47,49,63,120,123,125}	Rest periods of 7-14s between loading cycles improved bone formation response. Optimal thresholds of rest periods should be determined for both mouse and rats studies.
Duration of loading	Multiple ^{17,20,34,37}	Multiple ^{19,24,47-50}	Single duration axial loading protocols were used to study acute response such as gene expression and histomorphometric changes. Multiple duration axial loading protocols applied three times a week for two weeks allow sufficient changes in bone mass and structure that can be studied with high resolution techniques such as micro CT.
Age	Young versus aged ³⁵	Young versus aged ^{67,71,72,74,118,156}	Aged mice were less mechanoresponsive than young mice, as loading-induced bone formation was lower in aged mice than in young mice.
Ovariectomy (OVX)	OVX versus sham ^{42,44}	OVX versus sham ^{22,28,92}	Axial loading did not prevent OVX induced bone loss in both rats and mice. Loading combined with tamoxifen treatment improved bone mass in mice studies. The effect of axial loading should be studied in conditions of sex-steroid treatment in OVX rats and mice.
Sciatic Neurectomy (SN)	NA	SN versus controls ^{32,77}	Disuse or sciatic neurectomy increased mechanosensitivity as compared to controls, suggesting bone mass improvement with loading in space flights or during long-term disuse.
Interventions	Bisphosphonates ⁴² , COX-2 inhibitor NS398 ³⁸ , verapamil ⁴⁰ , PTH ⁴⁰ , ultrasound ³¹	Tamoxifen ²⁸ , CXCR4 antagonist AMD3100 ⁵⁰ , PTH ^{126,127,131} , Prednisolone ⁴⁶ , Gambogic amide ¹⁰⁵	Bisphosphonate treatment improved mechanoresponse in both OVX rats and mice. Axial loading induced bone formation was suppressed by COX-2 inhibitor indomethacin or NS398 treatment in rats. Verapamil treatment suppressed loading-induced bone formation. PTH treatment improved loading-induced bone formation in both rats and mice. Axial loading-induced bone formation was improved by ultrasound in rats. CCRX4 agonist AMD3100 suppressed axial loading-induced bone formation in mice. Gambogic amide was associated with load-induced increase in periosteal bone formation rate.

change in these parameters in loading protocols affects bone formation^{9,37}. A frequency of 2 Hz, which was a common frequency reported in the articles from this review was shown to be equivalent to a normal stride frequency observed during locomotion¹⁷, although a frequency of 5-10 Hz was shown to have a larger effect on bone formation, but bone formation plateaued above 10 Hz frequency⁵⁷. Strain must reach a certain magnitude above MES for bone formation³⁻⁶. The difference between the MES and a strain causing negative effects, such as woven bone formation, may be rather small and should be noticed⁴⁸. Rest periods between loading cycles were also thought to enhance bone formation³¹, but evidence using controlled axial loading experiments is lacking.

Other factors have been examined to determine the influence on mechano-adaptation. Axial loading studies commonly used Sprague Dawley rats. Species-related differences in axial loading-related bone outcomes were not reported, suggesting similarity in bone mass and structure among the different rat species. Additionally, aging did not seem to affect mechanoresponse to axial loading in one rat study³⁵. Though, mechanoresponse decreased in aged rats as compared to younger rats using a four-point bending model⁸⁹. Age is therefore still considered an important modifying factor that may influence the bone outcomes. The relationship between age and mechanoresponsiveness can likely be explained by the age-related decline in certain cell

types—osteoblasts, osteocytes and lining cells—that sense mechanical signals⁹⁰, thereby reducing the mechanosensing ability of bone. Age related decline was reported in IGF-1 and binding proteins⁹¹. IGF-1 levels are associated with bone formation response, as IGF-1 stimulates osteoblastic activity⁹¹. Sex-steroid deficient rat models (OVX, ORX) were often used since they induce osteoporotic conditions and axial loading was investigated for prevention of bone loss or restoration of bone mass^{42,43}. Although ovariectomized rats did not show overall differences in bone mass increase in response to loading as compared to controls^{42,92}, axial loading may be beneficial for OVX-induced osteoporosis in cases of low bone volume⁴³.

Mechanical loading protocols and modifying factors affecting loading related bone outcomes in mouse and knock out mouse models

In mouse studies, peak load, loading cycles, frequency, and rest periods were the main methodological determinants of bone outcomes. Load was mostly calculated on the basis of induced strain, which was determined through load-strain calibration using strain gauges or using a micro CT-derived computational method to determine site-specific strain in mouse tibia^{21,22}. Additionally, axial loading of a mouse tibia or ulna also caused bending of the bone which is different on lateral and medial or anterior and posterior sides, leading to different strains on periosteal and endocortical surfaces⁴⁸. Strain requirements for KO mice were always different from control mice due to bone phenotype with altered bone strength. Change in frequency or number of cycles applied with the different peak loads influenced outcomes of bone mass, structure, and density in the different loading protocols^{52,57}. This indicates that from the methodological aspects, both number of loading cycles and peak loads are important parameters in the loading protocols that affect bone outcomes. However, a minimal number of loading cycles should be used, as a range of loading cycles from 60-1200 showed a similar bone formation response to loading⁵², and a large number of load cycles may unnecessarily prolong loading experiments causing anesthesia related side-effects⁵². A rest period of ten seconds between loading cycles was sometimes applied to improve bone outcomes in mice. Evidence for a beneficial effect of including rest periods and the optimal duration of a rest period is lacking, since none of these studies were done with appropriate non-rest controls.

Aged mice showed reduced mechanoresponsiveness, as compared to young mice^{71,93}. Although mechanoresponsiveness is diminished in aged mice, mechanical loading increased cortical bone volume in both young mice, adult mice, and older mice⁹³. Thus, axial loading in adult mice may be a suitable model to study whether mechanical loading or exercise can prevent age-related bone loss. OVX mice responded to loading similarly as controls, whereas tamoxifen-treated OVX mice showed improved bone formation after loading as compared to non-tamoxifen-treated OVX mice. This agrees with previous studies in rodent

models⁹⁴ and also in postmenopausal women⁹⁵, where bone mineral density improved with a combination of exercise and hormonal replacement. Tamoxifen is also used in conditional gene inactivation, (based on the DNA recombinase Cre and its recognition (loxP) sites), in mice to switch on or off the gene of interest⁹⁶. It is in these animal models important to realize that tamoxifen might act as a confounder when investigating bone mechanoresponse⁹⁶. Taken together, this implies that both age and estrogen status are important modifying factors in mice axial loading. Axial loading restored the cortical bone loss induced by sciatic neurectomy by increasing bone formation both in both short or long-term³², which implies that loading after a period of disuse is not only useful to increase the effect size but may also be helpful to investigate conditions of disuse osteoporosis^{32,76,77}. Sciatic neurectomy reduced bone mass by decreasing osteoblasts activity through adrenergic receptors present in these cells³². However, the mechanism of disuse-related rejuvenation in neurectomized aged rats is not clear. Neurectomy-related muscle catabolism which activates growth factors such as latent TGF- β may stimulate bone formation in aged-mice and disuse may activate periosteal and endosteal osteoblast function⁷⁸.

Since different studies have different objectives, a variety of loading protocols, outcome parameters and modifying factors will always be practiced. This review puts the methodological aspects of loading parameters and factors that can influence the different bone outcomes into perspective. This may help the interpretation of the many papers that published data on mechano-adaptation. The papers on methodological aspects affecting mechanical loading-related bone outcomes outlined in this study can also be helpful for future investigators when designing their loading protocols. Therefore, in this review, we summarized some general suggestions for rat and mouse axial loading protocols in Table 4. Frequently reported values of loading parameters including: peak load, strain, frequency, number of cycles and rest periods in the selected rat ulna, mice ulna and tibia studies, and effects of commonly used modifying factors, such as age, sex-steroid deficiency, and disuse are summarized in Table 4.

Conclusion

In conclusion, this review shows that peak load, loading cycles, loading frequency are the major methodological determinants of loading-induced outcomes of bone mass, structure, and density in rat and mouse axial loading studies. The effective window between MES and the strain that causes side effects such as woven bone due to rapid bone formation may be rather small. Therefore, the peak strain magnitude should be chosen carefully to avoid negative effects such as woven bone formation. Application of rest periods in loading protocols should be further investigated by introducing appropriate controls without rest insertion between loading cycles. In addition, micro CT- derived computational techniques have shown to accurately calculate optimal strain

for bone formation at different sites in rat and mouse axial loading studies. These techniques are preferred since they reduce animal discomfort. In order to compare data on mechanoreponse and predict effects on bone outcomes, it is important to account for the methodological aspects of loading including load, strain, frequency, and number of cycles, especially in the context of modifying factors which may alter bone formation, such as age, sex-steroid deficiency and antecedent periods of disuse.

Funding

This study was funded by the European Commission through MOVE-AGE, an Erasmus Mundus Joint Doctorate program (2011–2015).

Authors' contributions

AKN, NB and PL did the conception or design of the work. AKN, HWE, NB and RO did the acquisition, analysis, or interpretation of data. AKN drafted the manuscript, HWE, RJ, NS, RO, DV, PL and NB revising it critically for important intellectual content; AND AKN, HWE, RJ, NS, RO, DV, PL and NB approved the final version to be published.

References

- Lanyon LE. Using functional loading to influence bone mass and architecture: objectives, mechanisms, and relationship with estrogen of the mechanically adaptive process in bone. *Bone* 1996;18(1 Suppl):37s-43s.
- Ehrlich PJ, Lanyon LE. Mechanical strain and bone cell function: a review. *Osteoporos Int* 2002;13(9):688-700.
- Frost HM. Defining osteopenias and osteoporosis: another view (with insights from a new paradigm). *Bone* 1997;20(5):385-91.
- Frost HM. The Utah paradigm of skeletal physiology: an overview of its insights for bone, cartilage and collagenous tissue organs. *J Bone Miner Metab* 2000; 18(6):305-16.
- Frost HM. The Utah paradigm of Skeletal Physiology. vol 1. Bone and Bones and Associated Problems. ISMNI; 2004.
- Frost HM. The Utah paradigm of Skeletal Physiology. vol 2. Bone and Bones and Associated Problems. ISMNI; 2004.
- Meakin LB, Price JS, Lanyon LE. The Contribution of Experimental *in vivo* Models to Understanding the Mechanisms of Adaptation to Mechanical Loading in Bone. *Front Endocrinol (Lausanne)* 2014;5:154.
- Wittkowske C, Reilly GC, Lacroix D, Perrault CM. *In Vitro* Bone Cell Models: Impact of Fluid Shear Stress on Bone Formation. *Front Bioeng Biotechnol* 2016;4:87.
- Torrance AG, Mosley JR, Suswillo RF, Lanyon LE. Noninvasive loading of the rat ulna *in vivo* induces a strain-related modeling response uncomplicated by trauma or periosteal pressure. *Calcif Tissue Int* 1994; 54(3):241-7.
- Srinivasan S, Weimer DA, Agans SC, Bain SD, Gross TS. Low-magnitude mechanical loading becomes osteogenic when rest is inserted between each load cycle. *J Bone Miner Res* 2002;17(9):1613-20.
- Stadelmann VA, Brun J, Bonnet N. Preclinical mouse models for assessing axial compression of long bones during exercise. *Bonekey Rep* 2015;4:768.
- McBride SH, Silva MJ. Adaptive and Injury Response of Bone to Mechanical Loading. *Bonekey Osteovision* 2012;1:192.
- Melville KM, Robling AG, van der Meulen MC. *In vivo* axial loading of the mouse tibia. *Methods Mol Biol* 2015; 1226:99-115.
- Moher D, Liberati A, Tetzlaff J, Altman DG, Group P. Preferred reporting items for systematic reviews and meta-analyses: the PRISMA statement. *BMJ* 2009; 339:b2535.
- Sophocleous A, Idris AI. Rodent models of osteoporosis. *Bonekey Rep* 2014;3:614.
- Meakin LB, Sugiyama T, Galea GL, Browne WJ, Lanyon LE, Price JS. Male mice housed in groups engage in frequent fighting and show a lower response to additional bone loading than females or individually housed males that do not fight. *Bone* 2013;54(1):113-7.
- Mosley JR, Lanyon LE. Strain rate as a controlling influence on adaptive modeling in response to dynamic loading of the ulna in growing male rats. *Bone* 1998; 23(4):313-8.
- Begonia M, Dallas M, Johnson ML, Thiagarajan G. Comparison of strain measurement in the mouse forearm using subject-specific finite element models, strain gaging, and digital image correlation. *Biomechanics and modeling in mechanobiology* 2017;16(4):1243-1253.
- Kuruvilla SJ, Fox SD, Cullen DM, Akhter MP. Site specific bone adaptation response to mechanical loading. *J Musculoskelet Neuronal Interact* 2008;8(1):71-8.
- Hsieh YF, Robling AG, Ambrosius WT, Burr DB, Turner CH. Mechanical loading of diaphyseal bone *in vivo*: the strain threshold for an osteogenic response varies with location. *J Bone Miner Res* 2001;16(12):2291-7.
- Norman SC, Wagner DW, Beaupre GS, Castillo AB. Comparison of three methods of calculating strain in the mouse ulna in exogenous loading studies. *J Biomech* 2015;48(1):53-8.
- Li H, Li RX, Wan ZM, et al. Counter-effect of constrained dynamic loading on osteoporosis in ovariectomized mice. *J Biomech* 2013;46(7):1242-7.
- Zhao L, Dodge T, Nemani A, Yokota H. Resonance in the mouse tibia as a predictor of frequencies and locations of loading-induced bone formation. *Biomech Model Mechanobiol* 2014;13(1):141-51.
- Robling AG, Hinant FM, Burr DB, Turner CH. Shorter, more frequent mechanical loading sessions enhance bone mass. *Medicine and science in sports and exercise* 2002;34(2):196-202.
- Warden SJ, Hurst JA, Sanders MS, Turner CH, Burr DB, Li J. Bone adaptation to a mechanical loading program significantly increases skeletal fatigue resistance. *J Bone Miner Res* 2005;20(5):809-16.

26. Kumar R, Tiwari AK, Tripathi D, Shrivastava NV, Nizam F. Canalicular fluid flow induced by loading waveforms: A comparative analysis. *J Theor Biol* 2019;471:59-73.
27. Robling AG, Duijvelaar KM, Geevers JV, Ohashi N, Turner CH. Modulation of appositional and longitudinal bone growth in the rat ulna by applied static and dynamic force. *Bone* 2001;29(2):105-13.
28. Sugiyama T, Galea GL, Lanyon LE, Price JS. Mechanical loading-related bone gain is enhanced by tamoxifen but unaffected by fulvestrant in female mice. *Endocrinology* 2010;151(12):5582-90.
29. Sugiyama T, Meakin LB, Galea GL, et al. Risedronate does not reduce mechanical loading-related increases in cortical and trabecular bone mass in mice. *Bone* 2011;49(1):133-9.
30. Sugiyama T, Saxon LK, Zaman G, et al. Mechanical loading enhances the anabolic effects of intermittent parathyroid hormone (1-34) on trabecular and cortical bone in mice. *Bone* 2008;43(2):238-48.
31. Perry MJ, Parry LK, Burton VJ, et al. Ultrasound mimics the effect of mechanical loading on bone formation *in vivo* on rat ulnae. *Med Eng Phys* 2009;31(1):42-7.
32. de Souza RL, Pitsillides AA, Lanyon LE, Skerry TM, Chenu C. Sympathetic nervous system does not mediate the load-induced cortical new bone formation. *J Bone Miner Res* 2005;20(12):2159-68.
33. Li Y, de Bakker CMJ, Lai X, et al. Maternal bone adaptation to mechanical loading during pregnancy, lactation, and post-weaning recovery. *Bone* 2021;151:116031.
34. Hsieh YF, Turner CH. Effects of loading frequency on mechanically induced bone formation. *J Bone Miner Res* 2001;16(5):918-24.
35. Saxon LK, Robling AG, Alam I, Turner CH. Mechanosensitivity of the rat skeleton decreases after a long period of loading, but is improved with time off. *Bone* 2005;36(3):454-64.
36. Saxon LK, Turner CH. Low-dose estrogen treatment suppresses periosteal bone formation in response to mechanical loading. *Bone* 2006;39(6):1261-7.
37. Chen Xy, Zhang Xz, Guo Y, Li Rx, Lin Jj, Wei Y. The establishment of a mechanobiology model of bone and functional adaptation in response to mechanical loading. *Clinical Biomechanics* 2008;23(SUPPL.1):S88-S95.
38. Li J, Burr DB, Turner CH. Suppression of prostaglandin synthesis with NS-398 has different effects on endocortical and periosteal bone formation induced by mechanical loading. *Calcif Tissue Int* 2002;70(4):320-9.
39. Tomlinson RE, Schmieder AH, Quirk JD, Lanza GM, Silva MJ. Antagonizing the $\alpha v \beta 3$ integrin inhibits angiogenesis and impairs woven but not lamellar bone formation induced by mechanical loading. *Journal of Bone and Mineral Research* 29(9):1970-1980.
40. Li J, Duncan RL, Burr DB, Gattone VH, Turner CH. Parathyroid hormone enhances mechanically induced bone formation, possibly involving L-type voltage-sensitive calcium channels. *Endocrinology* 2003;144(4):1226-33.
41. Warden SJ, Fuchs RK, Castillo AB, Nelson IR, Turner CH. Exercise when young provides lifelong benefits to bone structure and strength. *J Bone Miner Res* 2007;22(2):251-9.
42. Feher A, Koivunemi A, Koivunemi M, et al. Bisphosphonates do not inhibit periosteal bone formation in estrogen deficient animals and allow enhanced bone modeling in response to mechanical loading. *Bone* 2010;46(1):203-7.
43. Ko CY, Jung YJ, Park JH, et al. Trabecular bone response to mechanical loading in ovariectomized Sprague-Dawley rats depends on baseline bone quantity. *J Biomech* 2012;45(11):2046-9.
44. Warden SJ, Galley MR, Hurd AL, et al. Elevated mechanical loading when young provides lifelong benefits to cortical bone properties in female rats independent of a surgically induced menopause. *Endocrinology* 2013;154(9):3178-87.
45. Yang PF, Huang LW, Nie XT, et al. Moderate tibia axial loading promotes discordant response of bone composition parameters and mechanical properties in a hindlimb unloading rat model. *J Musculoskeletal Neuronal Interact* 2018;18(2):152-164.
46. Bergstrom I, Isaksson H, Koskela A, et al. Prednisolone treatment reduces the osteogenic effects of loading in mice. *Bone* 2018;112:10-18.
47. Moustafa A, Sugiyama T, Prasad J, et al. Mechanical loading-related changes in osteocyte sclerostin expression in mice are more closely associated with the subsequent osteogenic response than the peak strains engendered. *Osteoporos Int* 2012;23(4):1225-34. doi:10.1007/s00198-011-1656-4
48. Berman AG, Clauser CA, Wunderlin C, Hammond MA, Wallace JM. Structural and Mechanical Improvements to Bone Are Strain Dependent with Axial Compression of the Tibia in Female C57BL/6 Mice. *PLoS One* 2015;10(6):e0130504.
49. Holquin N, Brodt MD, Sanchez ME, Kotiya AA, Silva MJ. Adaptation of tibial structure and strength to axial compression depends on loading history in both C57BL/6 and BALB/c mice. *Calcif Tissue Int* 2013;93(3):211-21.
50. Leucht P, Temiyasathit S, Russell A, et al. CXCR4 antagonism attenuates load-induced periosteal bone formation in mice. *J Orthop Res* 2013;31(11):1828-38.
51. Kang KS, Hong JM, Robling AG. Postnatal beta-catenin deletion from Dmp1-expressing osteocytes/osteoblasts reduces structural adaptation to loading, but not periosteal load-induced bone formation. *Bone* 2016;88:138-45.
52. Sun D, Brodt MD, Zannit HM, Holquin N, Silva MJ. Evaluation of loading parameters for murine axial tibial loading: Stimulating cortical bone formation while reducing loading duration. *J Orthop Res* 2018;36(2):682-691.
53. Birkhold AI, Razi H, Duda GN, Checa S, Willie BM.

- Tomography-Based Quantification of Regional Differences in Cortical Bone Surface Remodeling and Mechano-Response. *Calcified tissue international* 2016;100(3):255-270.
54. Grimston SK, Watkins MP, Brodt MD, Silva MJ, Civitelli R. Enhanced periosteal and endocortical responses to axial tibial compression loading in conditional connexin43 deficient mice. *PLoS One* 2012;7(9):e44222.
 55. Bivi N, Pacheco-Costa R, Brun LR, et al. Absence of Cx43 selectively from osteocytes enhances responsiveness to mechanical force in mice. *J Orthop Res* 2013;31(7):1075-81.
 56. Parajuli A, Liu C, Li W, et al. Bone's responses to mechanical loading are impaired in type 1 diabetes. *Bone* 2015;81:152-60.
 57. Warden SJ, Turner CH. Mechanotransduction in the cortical bone is most efficient at loading frequencies of 5-10 Hz. *Bone* 2004;34(2):261-70.
 58. Bonnet N, Standley KN, Bianchi EN, et al. The matricellular protein periostin is required for sost inhibition and the anabolic response to mechanical loading and physical activity. *J Biol Chem* 2009;284(51):35939-50.
 59. Callewaert F, Bakker A, Schrooten J, et al. Androgen Receptor Disruption Increases the Osteogenic Response to Mechanical Loading in Male Mice. *Journal of Bone & Mineral Research* 2010;25(1):124-131.
 60. Kesavan C, Wergedal JE, William Lau KH, Mohan S. Conditional disruption of IGF-I gene in type 1(alpha) collagen-expressing cells shows an essential role of IGF-I in skeletal anabolic response to loading. *American Journal of Physiology - Endocrinology and Metabolism* 2011;301(6):E1191-E1197.
 61. Sinnesael M, Claessens F, Laurent M, et al. Androgen receptor (AR) in osteocytes is important for the maintenance of male skeletal integrity: evidence from targeted AR disruption in mouse osteocytes. *J Bone Miner Res* 2012;27(12):2535-43.
 62. Fritton JC, Myers ER, Wright TM, van der Meulen MC. Loading induces site-specific increases in mineral content assessed by microcomputed tomography of the mouse tibia. *Bone* 2005;36(6):1030-8.
 63. Sugiyama T, Price JS, Lanyon LE. Functional adaptation to mechanical loading in both cortical and cancellous bone is controlled locally and is confined to the loaded bones. *Bone* 2010;46(2):314-21.
 64. Galea GL, Hannuna S, Meakin LB, Delisser PJ, Lanyon LE, Price JS. Quantification of Alterations in Cortical Bone Geometry Using Site Specificity Software in Mouse models of Aging and the Responses to Ovariectomy and Altered Loading. *Front Endocrinol (Lausanne)* 2015; 6:52.
 65. Fritton JC, Myers ER, Wright TM, van der Meulen MC. Bone mass is preserved and cancellous architecture altered due to cyclic loading of the mouse tibia after orchidectomy. *J Bone Miner Res* 2008;23(5):663-71.
 66. De Souza RL, Matsuura M, Eckstein F, Rawlinson SC, Lanyon LE, Pitsillides AA. Non-invasive axial loading of mouse tibiae increases cortical bone formation and modifies trabecular organization: a new model to study cortical and cancellous compartments in a single loaded element. *Bone* 2005;37(6):810-8.
 67. Holguin N, Brodt MD, Sanchez ME, Silva MJ. Aging diminishes lamellar and woven bone formation induced by tibial compression in adult C57BL/6. *Bone* 2014;65:83-91.
 68. Meakin LB, Galea GL, Sugiyama T, Lanyon LE, Price JS. Age-related impairment of bones' adaptive response to loading in mice is associated with sex-related deficiencies in osteoblasts but no change in osteocytes. *J Bone Miner Res* 2014;29(8):1859-71.
 69. Yang H, Embry RE, Main RP. Effects of Loading Duration and Short Rest Insertion on Cancellous and Cortical Bone Adaptation in the Mouse Tibia. *PLoS One* 2017;12(1):e0169519. doi:10.1371/journal.pone.0169519
 70. Robling AG, Turner CH. Mechanotransduction in bone: genetic effects on mechanosensitivity in mice. *Bone* 2002;31(5):562-9.
 71. Aido M, Kerschnitzki M, Hoerth R, et al. Effect of *in vivo* loading on bone composition varies with animal age. *Exp Gerontol* 2015;63:48-58.
 72. Willie BM, Birkhold AI, Razi H, et al. Diminished response to *in vivo* mechanical loading in trabecular and not cortical bone in adulthood of female C57Bl/6 mice coincides with a reduction in deformation to load. *Bone* 2013;55(2):335-46.
 73. Main RP. Load-induced changes in bone stiffness and cancellous and cortical bone mass following tibial compression diminish with age in female mice. *The Journal of experimental biology* 2014;217:1775-1783.
 74. Checa S, Hesse B, Roschger P, et al. Skeletal maturation substantially affects elastic tissue properties in the endosteal and periosteal regions of loaded mice tibiae. *Acta Biomater* 2015;21:154-164.
 75. Saxon LK, Robling AG, Castillo AB, Mohan S, Turner CH. The skeletal responsiveness to mechanical loading is enhanced in mice with a null mutation in estrogen receptor-(beta). *American Journal of Physiology - Endocrinology and Metabolism* 2007; 293(2):E484-E491.
 76. Meakin LB, Delisser PJ, Galea GL, Lanyon LE, Price JS. Disuse rescues the age-impaired adaptive response to external loading in mice. *Osteoporos Int* 2015; 26(11):2703-8.
 77. DeSouza R, Javaheri B, Collinson RS, et al. Prolonging disuse in aged mice amplifies cortical but not trabecular bones' response to mechanical loading. *J Musculoskelet Neuronal Interact* 2017;17(3):218-225.
 78. Galea GL, Delisser PJ, Meakin L, Price JS, Windahl SH. Bone gain following loading is site-specifically enhanced by prior and concurrent disuse in aged male mice. *Bone* 2020;133:115255.
 79. Bouchard AL, Dsouza C, Julien C, et al. Bone adaptation to mechanical loading in mice is affected by circadian

- rhythms. *Bone* 2022;154:116218.
80. Windahl SH, Borjesson AE, Farman HH, et al. Estrogen receptor-alpha in osteocytes is important for trabecular bone formation in male mice. *Proceedings of the National Academy of Sciences of the United States of America* 2013;110(6):2294-9.
 81. Melville KM, Kelly NH, Surita G, et al. Effects of Deletion of ERalpha in Osteoblast-Lineage Cells on Bone Mass and Adaptation to Mechanical Loading Differ in Female and Male Mice. *J Bone Miner Res* 2015;30(8):1468-80.
 82. Lee KCL, Jessop H, Suswillo R, Zaman G, Lanyon LE. The adaptive response of bone to mechanical loading in female transgenic mice is deficient in the absence of oestrogen receptor-(alpha) and -(beta). *Journal of Endocrinology* 2004;182(2):193-201.
 83. Saxon LK, Robling AG, Castillo AB, Mohan S, Turner CH. The skeletal responsiveness to mechanical loading is enhanced in mice with a null mutation in estrogen receptor-beta. *Am J Physiol Endocrinol Metab* 2007;293(2):E484-91.
 84. Lee KC, Jessop H, Suswillo R, Zaman G, Lanyon LE. The adaptive response of bone to mechanical loading in female transgenic mice is deficient in the absence of oestrogen receptor-alpha and -beta. *J Endocrinol* 2004;182(2):193-201.
 85. Sugiyama T, Meakin LB, Galea GL, Lanyon LE, Price JS. The cyclooxygenase-2 selective inhibitor NS-398 does not influence trabecular or cortical bone gain resulting from repeated mechanical loading in female mice. *Osteoporos Int* 2013;24(1):383-8.
 86. Tu X, Rhee Y, Condon KW, et al. Sost downregulation and local Wnt signaling are required for the osteogenic response to mechanical loading. *Bone* 2012;50(1):209-17.
 87. Tomlinson RE, Li Z, Li Z, et al. NGF-TrkA signaling in sensory nerves is required for skeletal adaptation to mechanical loads in mice. *Proceedings of the National Academy of Sciences of the United States of America* 2017;114(18):E3632-E3641.
 88. Kotha SP, Hsieh YF, Strigel RM, Muller R, Silva MJ. Experimental and finite element analysis of the rat ulnar loading model-correlations between strain and bone formation following fatigue loading. *J Biomech* 2004;37(4):541-8.
 89. Turner CH, Takano Y, Owan I. Aging changes mechanical loading thresholds for bone formation in rats. *J Bone Miner Res* 1995;10(10):1544-9.
 90. Kita K, Kawai K, Hirohata K. Changes in bone marrow blood flow with aging. *J Orthop Res* 1987;5(4):569-75.
 91. Benedict MR, Adiyaman S, Ayers DC, et al. Dissociation of bone mineral density from age-related decreases in insulin-like growth factor-I and its binding proteins in the male rat. *J Gerontol* 1994;49(5):B224-30.
 92. Warden SJ, Galley MR, Hurd AL, et al. Cortical and trabecular bone benefits of mechanical loading are maintained long term in mice independent of ovariectomy. *J Bone Miner Res* 2014;29(5):1131-40.
 93. Birkhold AI, Razi H, Duda GN, Weinkamer R, Checa S, Willie BM. Mineralizing surface is the main target of mechanical stimulation independent of age: 3D dynamic *in vivo* morphometry. *Bone* 2014;66:15-25.
 94. Tromp AM, Bravenboer N, Tanck E, et al. Additional weight bearing during exercise and estrogen in the rat: the effect on bone mass, turnover, and structure. *Calcif Tissue Int* 2006;79(6):404-15.
 95. Kohrt WM, Snead DB, Slatopolsky E, Birge SJ, Jr. Additive effects of weight-bearing exercise and estrogen on bone mineral density in older women. *J Bone Miner Res* 1995;10(9):1303-11.
 96. Friedel RH, Wurst W, Wefers B, Kühn R. Generating conditional knockout mice. *Methods Mol Biol* 2011;693:205-31.
 97. Mustafy T, Londono I, Moldovan F, Villemure I. Isolated Cyclic Loading During Adolescence Improves Tibial Bone Microstructure and Strength at Adulthood. *JBM Plus* 2020;4(4):e10349.
 98. Noble BS, Peet N, Stevens HY, et al. Mechanical loading: biphasic osteocyte survival and targeting of osteoclasts for bone destruction in rat cortical bone. *Am J Physiol Cell Physiol* 2003;284(4):C934-43.
 99. Schriefer JL, Robling AG, Warden SJ, Fournier AJ, Mason JJ, Turner CH. A comparison of mechanical properties derived from multiple skeletal sites in mice. *Journal of Biomechanics* 2005;38(3):467-475.
 100. Berman AG, Hinton MJ, Wallace JM. Treadmill running and targeted tibial loading differentially improve bone mass in mice. *Bone Rep* 2019;10:100195.
 101. Cheong VS, Kadirkamanathan V, Dall'Ara E. The Role of the Loading Condition in Predictions of Bone Adaptation in a Mouse Tibial Loading Model. *Front Bioeng Biotechnol* 2021;9:676867.
 102. Cheong VS, Roberts BC, Kadirkamanathan V, Dall'Ara E. Bone remodelling in the mouse tibia is spatio-temporally modulated by oestrogen deficiency and external mechanical loading: A combined *in vivo/in silico* study. *Acta Biomater* 2020;116:302-317.
 103. Cheong VS, Roberts BC, Kadirkamanathan V, Dall'Ara E. Positive interactions of mechanical loading and PTH treatments on spatio-temporal bone remodelling. *Acta Biomater* 2021;136:291-305.
 104. DeLong A, Friedman MA, Tucker SM, et al. Protective Effects of Controlled Mechanical Loading of Bone in C57BL6/J Mice Subject to Disuse. *JBM Plus* 2020;4(3):e10322.
 105. Fioravanti G, Hua PQ, Tomlinson RE. The TrkA agonist gambogic amide augments skeletal adaptation to mechanical loading. *Bone* 2021;147:115908.
 106. Gohin S, Javaheri B, Hopkinson M, Pitsillides AA, Arnett TR, Chenu C. Applied mechanical loading to mouse hindlimb acutely increases skeletal perfusion and chronically enhanced vascular porosity. *J Appl Physiol* (1985) 2020;128(4):838-846.
 107. Ko FC, Dragomir CL, Plumb DA, et al. Progressive cell-mediated changes in articular cartilage and bone in

- mice are initiated by a single session of controlled cyclic compressive loading. *J Orthop Res* 2016;34(11):1941-1949.
108. Krause AR, Speacht TA, Steiner JL, Lang CH, Donahue HJ. Mechanical loading recovers bone but not muscle lost during unloading. *NPJ Microgravity* 2020;6(1):36.
 109. Lee KC, Maxwell A, Lanyon LE. Validation of a technique for studying functional adaptation of the mouse ulna in response to mechanical loading. *Bone* 2002;31(3):407-12.
 110. Lionikaite V, Henning P, Drevinge C, et al. Vitamin A decreases the anabolic bone response to mechanical loading by suppressing bone formation. *FASEB J* 2019;33(4):5237-5247.
 111. Lynch ME, Main RP, Xu Q, et al. Cancellous bone adaptation to tibial compression is not sex dependent in growing mice. *Journal of Applied Physiology* 2010;109(3):685-691.
 112. Lynch MA, Brodt MD, Stephens AL, Civitelli R, Silva MJ. Low-magnitude whole-body vibration does not enhance the anabolic skeletal effects of intermittent PTH in adult mice. *J Orthop Res* 2011;29(4):465-72.
 113. Miller CJ, Trichilo S, Pickering E, et al. Cortical Thickness Adaptive Response to Mechanical Loading Depends on Periosteal Position and Varies Linearly With Loading Magnitude. *Front Bioeng Biotechnol* 2021;9:671606.
 114. Park J, Fertala A, Tomlinson RE. Naproxen impairs load-induced bone formation, reduces bone toughness, and diminishes woven bone formation following stress fracture in mice. *Bone* 2019;124:22-32.
 115. Roberts BC, Arredondo Carrera HM, Zanjani-Pour S, et al. PTH(1-34) treatment and/or mechanical loading have different osteogenic effects on the trabecular and cortical bone in the ovariectomized C57BL/6 mouse. *Sci Rep* 2020;10(1):8889.
 116. Weatherholt AM, Fuchs RK, Warden SJ. Cortical and trabecular bone adaptation to incremental load magnitudes using the mouse tibial axial compression loading model. *Bone* 2013;52(1):372-9.
 117. Castillo AB, Alam I, Tanaka SM, et al. Low-amplitude, broad-frequency vibration effects on cortical bone formation in mice. *Bone* 2006;39(5):1087-96.
 118. Brodt MD, Silva MJ. Aged mice have enhanced endocortical response and normal periosteal response compared with young-adult mice following 1 week of axial tibial compression. *J Bone Miner Res* 2010;25(9):2006-15.
 119. Main RP, Lynch ME, van der Meulen MC. Load-induced changes in bone stiffness and cancellous and cortical bone mass following tibial compression diminish with age in female mice. *J Exp Biol* 2014;217(Pt 10):1775-83.
 120. Silva MJ, Brodt MD, Lynch MA, Stephens AL, Wood DJ, Civitelli R. Tibial loading increases osteogenic gene expression and cortical bone volume in mature and middle-aged mice. *PLoS One* 2012;7(4):e34980.
 121. Meakin LB, Udeh C, Galea GL, Lanyon LE, Price JS. Exercise does not enhance aged bone's impaired response to artificial loading in C57Bl/6 mice. *Bone* 2015;81:47-52.
 122. Shirazi-Fard Y, Alwood JS, Schreurs AS, Castillo AB, Globus RK. Mechanical loading causes site-specific anabolic effects on bone following exposure to ionizing radiation. *Bone* 2015;81:260-9.
 123. Sugiyama T, Meakin LB, Browne WJ, Galea GL, Price JS, Lanyon LE. Bones' adaptive response to mechanical loading is essentially linear between the low strains associated with disuse and the high strains associated with the lamellar/woven bone transition. *J Bone Miner Res* 2012;27(8):1784-93.
 124. Rapp AE, Bindl R, Heilmann A, et al. Systemic mesenchymal stem cell administration enhances bone formation in fracture repair but not load-induced bone formation. *Eur Cell Mater* 2015;29:22-34.
 125. Marenzana M, De Souza RL, Chenu C. Blockade of beta-adrenergic signaling does not influence the bone mechano-adaptive response in mice. *Bone* 2007;41(2):206-15.
 126. McAteer ME, Niziolek PJ, Ellis SN, Alge DL, Rob AG. Mechanical stimulation and intermittent parathyroid hormone treatment induce disproportional osteogenic, geometric, and biomechanical effects in growing mouse bone. *Calcified Tissue International* 2010;86(5):389-396.
 127. Moustafa A, Sugiyama T, Saxon LK, et al. The mouse fibula as a suitable bone for the study of functional adaptation to mechanical loading. *Bone* 2009;44(5):930-5.
 128. Stadelmann VA, Bonnet N, Pioletti DP. Combined effects of zoledronate and mechanical stimulation on bone adaptation in an axially loaded mouse tibia. *Clin Biomech (Bristol, Avon)* 2011;26(1):101-5.
 129. Borg SA, Buckley H, Owen R, et al. Early life vitamin D depletion alters the postnatal response to skeletal loading in growing and mature bone. *PLoS One* 2018;13(1):e0190675.
 130. Govey PM, Zhang Y, Donahue HJ. Mechanical Loading Attenuates Radiation-Induced Bone Loss in Bone Marrow Transplanted Mice. *PLoS One* 2016;11(12):e0167673.
 131. Meakin LB, Todd H, Delisser PJ, et al. Parathyroid hormone's enhancement of bones' osteogenic response to loading is affected by ageing in a dose- and time-dependent manner. *Bone* 2017;98:59-67.
 132. Heffner MA, Genetos DC, Christiansen BA. Bone adaptation to mechanical loading in a mouse model of reduced peripheral sensory nerve function. *PLoS One* 2017;12(10):e0187354.
 133. Wang QS, Wang GF, Lu YR, et al. The Combination of icariin and constrained dynamic loading stimulation attenuates bone loss in ovariectomy-induced osteoporotic mice. *J Orthop Res* 2018;36(5):1415-1424.
 134. Wang S, Pei S, Wasi M, et al. Moderate tibial loading and treadmill running, but not overloading, protect adult murine bone from destruction by metastasized breast

- cancer. *Bone* 2021;153:116100.
135. Yang H, Bullock WA, Myhal A, DeShield P, Duffy D, Main RP. Cancellous Bone May Have a Greater Adaptive Strain Threshold Than Cortical Bone. *JBMR Plus* 2021;5(5):e10489.
 136. Lu Y, Zuo D, Li J, He Y. Stochastic analysis of a heterogeneous micro-finite element model of a mouse tibia. *Med Eng Phys* 2019;63:50-56.
 137. Ziouti F, Ebert R, Rummeler M, et al. NOTCH Signaling Is Activated through Mechanical Strain in Human Bone Marrow-Derived Mesenchymal Stromal Cells. *Stem Cells Int* 2019;2019:5150634. doi:10.1155/2019/5150634
 138. Javaheri B, Razi H, Gohin S, et al. Lasting organ-level bone mechanoadaptation is unrelated to local strain. *Sci Adv* 2020;6(10):eaax8301.
 139. Alam I, Warden SJ, Robling AG, Turner CH. Mechanotransduction in bone does not require a functional cyclooxygenase-2 (COX-2) gene. *J Bone Miner Res* 2005;20(3):438-46.
 140. Castillo A, Mahaffey I, Cole W. Aging mice exhibit reduced periosteal and greater endosteal mechanoresponsiveness following two weeks of axial compressive loading. *Journal of Bone and Mineral Research* 2012;27.
 141. Javaheri B, Stern AR, Lara N, et al. Deletion of a single beta-catenin allele in osteocytes abolishes the bone anabolic response to loading. *J Bone Miner Res*. Mar 2014;29(3):705-15.
 142. Liedert A, Mattausch L, Rontgen V, et al. Midkine-deficiency increases the anabolic response of cortical bone to mechanical loading. *Bone* 2011;48(4):945-51.
 143. Litzenger JB, Tang WJ, Castillo AB, Jacobs CR. Deletion of (beta)1 integrins from cortical osteocytes reduces load-induced bone formation. *Cellular and Molecular Bioengineering* 2009;2(3):416-424.
 144. Morse A, McDonald MM, Kelly NH, et al. Mechanical load increases in bone formation via a sclerostin-independent pathway. *J Bone Miner Res* 2014;29(11):2456-67.
 145. Niziolek PJ, Warman ML, Robling AG. Mechanotransduction in bone tissue: The A214V and G171V mutations in Lrp5 enhance load-induced osteogenesis in a surface-selective manner. *Bone* 2012;51(3):459-65.
 146. Pierroz DD, Bonnet N, Bianchi EN, et al. Deletion of (beta)-adrenergic receptor 1, 2, or both leads to different bone phenotypes and response to mechanical stimulation. *Journal of Bone and Mineral Research* 2012;27(6):1252-1262.
 147. Robling AG, Warden SJ, Shultz KL, Beamer WG, Turner CH. Genetic effects on bone mechanotransduction in congenic mice harboring bone size and strength quantitative trait loci. *J Bone Miner Res* 2007; 22(7):984-91.
 148. Tomlinson RE, Silva MJ. HIF-1(alpha) regulates bone formation after osteogenic mechanical loading. *Bone* 2015;73:98-104.
 149. Wang N, Rumney RM, Yang L, et al. The P2Y(13) receptor regulates extracellular ATP metabolism and the osteogenic response to mechanical loading. *J Bone Miner Res* 2013;28(6):1446-56. doi:10.1002/jbmr.1877
 150. Zhao L, Shim JW, Dodge TR, Robling AG, Yokota H. Inactivation of Lrp5 in osteocytes reduces young's modulus and responsiveness to the mechanical loading. *Bone* 2013;54(1):35-43. doi:10.1016/j.bone.2013.01.033
 151. Svensson J, Windahl SH, Saxon L, et al. Liver-derived IGF-I regulates cortical bone mass but is dispensable for the osteogenic response to mechanical loading in female mice. *Am J Physiol Endocrinol Metab* 2016; 311(1):E138-44.
 152. Xiao Z, Dallas M, Qiu N, et al. Conditional deletion of Pkd1 in osteocytes disrupts skeletal mechanosensing in mice. *FASEB J* 2011;25(7):2418-32.
 153. Lories RJ, Peeters J, Bakker A, et al. Articular cartilage and biomechanical properties of the long bones in Frzb-knockout mice. *Arthritis Rheum* 2007;56(12):4095-103.
 154. Mohan S, Bhat CG, Wergedal JE, Kesavan C. *In vivo* evidence of IGF-I-estrogen crosstalk in mediating the cortical bone response to mechanical strain. *Bone Res* 2014;2:14007.
 155. Saxon LK, Jackson BF, Sugiyama T, Lanyon LE, Price JS. Analysis of multiple bone responses to graded strains above functional levels, and to disuse, in mice *in vivo* show that the human Lrp5 G171V High Bone Mass mutation increases the osteogenic response to loading but that lack of Lrp5 activity reduces it. *Bone* 2011;49(2):184-93.
 156. Pflanz D, Birkhold AI, Albiol L, et al. Sost deficiency led to a greater cortical bone formation response to mechanical loading and altered gene expression. *Sci Rep* 2017;7(1):9435.
 157. Moore ER, Zhu YX, Ryu HS, Jacobs CR. Periosteal progenitors contribute to load-induced bone formation in adult mice and require primary cilia to sense mechanical stimulation. *Stem Cell Res Ther* 2018;9(1):190.
 158. Robling AG, Kang KS, Bullock WA, et al. Sost, independent of the non-coding enhancer ECR5, is required for bone mechanoadaptation. *Bone* 2016;92:180-188.
 159. Sawakami K, Robling AG, Ai M, et al. The Wnt co-receptor LRP5 is essential for skeletal mechanotransduction but not for the anabolic bone response to parathyroid hormone treatment. *J Biol Chem* 2006;281(33):23698-711.
 160. Lee KL, Hoey DA, Spasic M, Tang T, Hammond HK, Jacobs CR. Adenylyl cyclase 6 mediates loading-induced bone adaptation *in vivo*. *FASEB J* 2014;28(3):1157-65.
 161. Sample SJ, Heaton CM, Behan M, et al. Role of calcitonin gene-related Peptide in functional adaptation of the skeleton. *PLoS One* 2014;9(12):e113959.
 162. Albiol L, Büttner A, Pflanz D, et al. Effects of Long-Term Sclerostin Deficiency on Trabecular Bone Mass and Adaption to Limb Loading Differ in Male and Female

- Mice. *Calcif Tissue Int* 2020;106(4):415-430.
163. Davis JL, Cox L, Shao C, et al. Conditional Activation of NF- κ B Inducing Kinase (NIK) in the Osteolineage Enhances Both Basal and Loading-Induced Bone Formation. *J Bone Miner Res* 2019;34(11):2087-2100.
164. Gerbaix M, Ammann P, Ferrari S. Mechanically Driven Counter-Regulation of Cortical Bone Formation in Response to Sclerostin-Neutralizing Antibodies. *J Bone Miner Res* 2021;36(2):385-399.
165. Lawson LY, Brodt MD, Migotsky N, Chermiside-Scabbo CJ, Palaniappan R, Silva MJ. Osteoblast-Specific Wnt Secretion Is Required for Skeletal Homeostasis and Loading-Induced Bone Formation in Adult Mice. *J Bone Miner Res* 2022;37(1):108-120.
166. Lewis KJ, Yi X, Wright CS, et al. The mTORC2 Component Rictor Is Required for Load-Induced Bone Formation in Late-Stage Skeletal Cells. *JBMR Plus* 2020;4(7):e10366.
167. Moore ER, Chen JC, Jacobs CR. Prx1-Expressing Progenitor Primary Cilia Mediate Bone Formation in response to Mechanical Loading in Mice. *Stem Cells Int* 2019;2019:3094154.
168. Morse A, Ko FC, McDonald MM, et al. Increased anabolic bone response in Dkk1 KO mice following tibial compressive loading. *Bone* 2020;131:115054.
169. Zannit HM, Brodt MD, Silva MJ. Proliferating osteoblasts are necessary for maximal bone anabolic response to loading in mice. *FASEB J* 2020;34(9):12739-12750.
170. Zannit HM, Silva MJ. Proliferation and Activation of Osterix-Lineage Cells Contribute to Loading-Induced Periosteal Bone Formation in Mice. *JBMR Plus* 2019; 3(11):e10227.